Available online at www.sciencedirect.com

SciVerse ScienceDirect

Procedia Engineering 00 (2012) 000–000

Procedia Engineering

www.elsevier.com/locate/procedia

5th BSME International Conference on Thermal Engineering

Experimental investigation into tribological characteristics of bio-lubricant formulated from Jatropha oil

M. Shahabuddin*, H.H. Masjuki, M.A. Kalam

Centre for Energy Sciences, Faculty of Engineering, University of Malaya, 50603 Kuala Lumpur, Malaysia

Abstract

The investigation of Lubricated Friction and Wear is an extended study. The aim of this study is to investigate the friction and wear characteristics of Jatropha oil based biolubricant by using Cygnus Wear Testing Machine under load of 30N, a high rotating speed of 2000 rpm and one hour operation time. In this study, SEA 40 was used as a reference base lubricant. As a biolubricant various blends like 10%, 20%, 30%, 40% and 50% of Jatropha oil were mixed with the base lubricant (SEA 40). The experiment was conducted using aluminium pins and cast iron disc which were lubricated with those of biolubricants. The lubricants were characterized by viscosity and elemental analysis using Viscometer and Multi oil analysers (MOA) respectively. To investigate wear and friction behaviour, image of worn surface have been taken by optical microscopy. From the experimental result, it is found that the lubricant regime that occurred during the experiment was boundary lubrication. The abrasive and the adhesive wear were the main wear mechanisms that occurred in the tests. The results of this experiment reveal that the addition of 10% jatropha oil with base lubricant can be used as lubricating oil without any shortcoming, which would help to reduce the global demand of petroleum based lubricant substantially.

Keywords: Biolubricant; lubrication; COF; wear; viscosity.

1. Introduction

Various types of lubricants are available all over the world including mineral oils, synthetic oils, re-refined oils, and vegetable oils. Most of the lubricants which are available in the market are based on mineral oil derived from petroleum oil which are not adaptable with the environment because of its toxicity and non-biodegradability [1, 2]. Unknown petroleum reserve and the increasing consumption, which made concern to use petroleum based lubricant thus, to find the alternative lubricant to meet the future demand is an important issue [3]. Therefore, vegetable oil can be played a vital role to substitute the petroleum lubricant as it possesses numerous advantage over base lubricant like renewability, environmentally friendly, biodegradability, less toxicity and so on [4-8]. It has been reported that yearly 12 million tons of lubricants waste are

* Corresponding Author: E-mail: shahabuddin.suzan@yahoo.com (M. Shahabuddin), Tel: +601-62418438, Fax: +603-79674448

released to the environment [9]. However, it is very difficult to dispose it safely for the mineral oil based lubricants due its toxic and non-biodegradable nature. To reduce the dependency on petroleum fuel, legislations have been passed to use certain percentage of biofuel in many countries, such initiative also required for lubricant as well [10]. Vegetable oils are mainly triglycerides which contain three hydroxyl groups and long chain unsaturated free fatty acids attached at the hydroxyl group by ester linkages acids favours triglycerides crystallization [11, 12]. The unsaturated free fatty acid which is defined as the ratio and position of carbon-carbon double bond, one two and three double bonds of carbon chain is named as a oleic, linoleic, and linolenic fatty acid components respectively [13]. The main limitations of vegetable oil are its poor low temperature behaviour, oxidation and thermal stability and gumming effect [14, 15]. These stabilities and pour point behaviour can be ameliorated by transesterification. Moreover the inferior flow property does not affect much in the tropical countries. Quinchia et al. [16] stated that, improving the potentiality of biolubricants some technical properties including available range of viscosities are need to improved. To do so, environmentally friendly viscosity modifier can be used. viscosity is the most important property for the lubricants since it determines the amount of friction that will be encountered between sliding surfaces and whether a thick enough film can be build up to avoid wear from solid-to-solid contact. Since little chance of viscosity with fluctuations in temperature is desirable to keep variations in friction at a minimum, fluid often are rated in terms of viscosity index. The less the viscosity is changed by temperature, the higher the viscosity index. Ethylene–vinyl acetate (EVA) and styrene–butadiene–styrene (SBS) copolymers were used to increase the viscosity range of high-oleic sunflower oil, in order to design new environmentally friendly lubricant formulations with increased viscosities. The maximum kinematic viscosities, at 40 and 100 ◦C, were increased up to around 150–250 cSt and 26–36 cSt, respectively [17].

Despite of having lot of advantages of biolubricant over petroleum based lubricant, the attempt to formulate the biolubricant and its applications are very few. Thus, in this article we sought to extend our investigation and to test the tribological characteristics and compatibility of non-edible Jatropha oil based biolubricant for the automotive application. The reason of selecting Jatropha oil as a base stock is it does not contend with the food and can be grown in marginal land.

2. Experimental

2.1 Lubricant sample preparation

There were six different types of lubricant sample were investigated in this study. The lubricant SAE 40 was used as a base lubricant and comparison purpose. Others samples were prepared by mixing of 10%, 20%, 30%, 40% and 50% Jatropha oil in SAE 40. The samples were mixed with the base lubricant by a homogeneous mixture machine.

2.2 Friction and wear evaluation

The apparatus used in the friction and wear testing process were Cygnus Friction and Wear Testing Machine which is connected with a personal computer (PC) with data acquisition system. It is a tri-pin-on-disc machine which is conducted by using three pins on a disc as testing specimens. Specifications of the Cygnus Test Machine are tabulated in Table 1. The block diagram of friction and wear testing are shown in Fig. 1. During the test the load of 30N and rotational speed of 2000 rpm were applied on pin.

Table 2 specification of Cygnus wear testing machine

Parameter	Value
Test Disc Diameter	110.0 mm
Test Pin Diameter	6.0 mm
Test Disc Speed Range	25 to 3000 rpm
Motor	Tuscan; (2000 rpm, 1.5 kW)
Load Range	0 KG to 30 KG
Electrical Input	220 Volt AC 50 Hz

2.3 Preparation of the Specimen

The specimens were prepared from aluminium and cast iron material. Aluminium was used to build three pin and cast iron is used for disc specimen. The construction geometry and the dimension are shown in Fig. 2. Prior to conduct the test it was ensured that the surface of the specimens are cleaned properly i. e, free from dirt and debris. Alcohol was used for cleaning purpose.

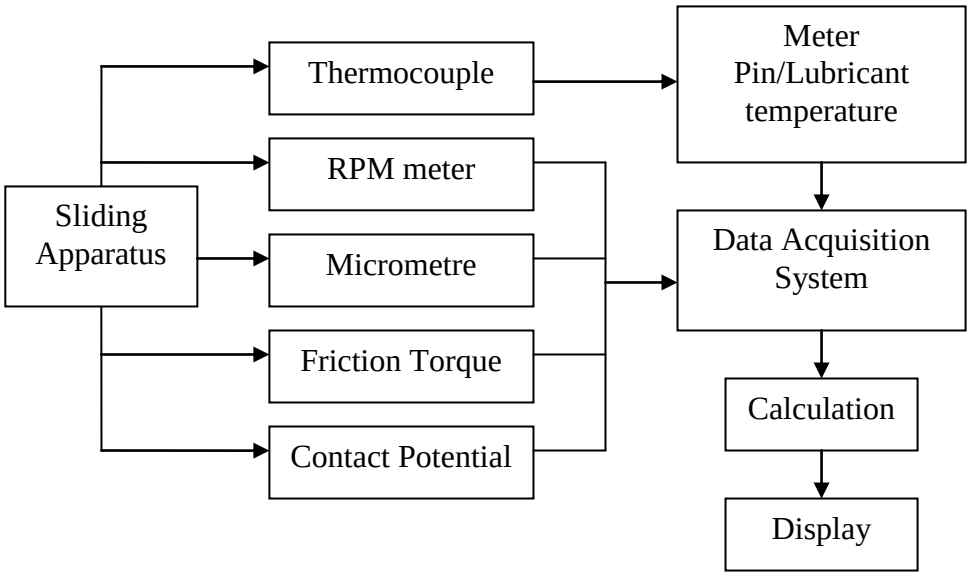

Fig.1. Block Diagrams of Friction and Wear Testing

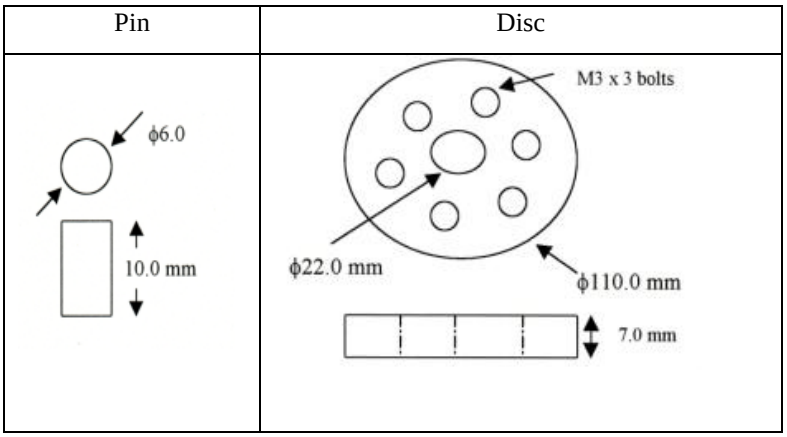

Fig.2. The dimensions and geometry's of pins and disc specimen

2.4 Lubricant analyses

Multi element oil analyser (MOA) was used to measure the wear elements in the lubricants by Atomic Emission Spectroscopy (AES). Whereas, for viscosity measurement the automatic Anton Paar viscosity meter was used with standard ASTM D 445. Viscosity was measured for both 40°C and 100°C controlled bath temperatures.

3 Results and discussion

3.1 Friction and Wear characterization

Fig. 3 show the pins wear as a function of sliding time for various Jatropha oil blended biolubricants. At the operating condition of 2000 rpm and 30 N loads, the linear pin wear varied from 0.02 to 0.05 mm. It is observed that the maximum wear occurred in the beginning of the experiment using biolubricants. It can be seen form the Fig. 3, that the maximum wear was occurred for JBL40 while the minimum wear was observed for JBL10. The results can be attributed to the maximum ability of the JBL 10 biolubricant film to protect metal to metal contact and keep consistency throughout the operation time while this ability is least for JBL40. It can also be seen that the rate of wear throughout the time is almost identical for the biolubricants whereas, the reducing trend is observed for the base lubricant. At the beginning of the test, the wear rate was very fast for few minutes which are known running-in period. During this period, the asperities of the sliding surface are cut off and the contact area of the sliding surface grows to an equilibrium size. After certain period of time, equilibrium wear condition between pins and disc surface was established and thereby the wear rate became steady. It can be identified from the Fig. 3 that the biolubricants JBL 30, JBL 40 and JBL 50 showed high wear while base lubricant, JBL 10 and JBL 20 impart low pin wear and their values are nearly same with each other.

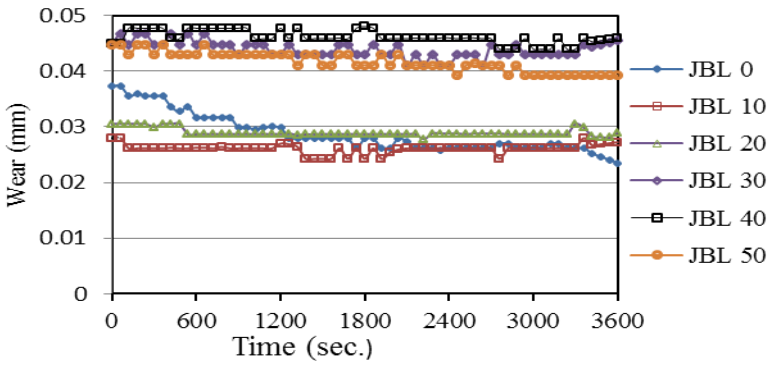

Fig.3. The linear pin wear as a function of sliding time for various Jatropha oil biolubricants.

Fig. 4 sows the loos of material from the pin for different percentage of biolubricant samples. It seems quite clear that the loos of material from the pins are highest for 50% biolubricant and that is least for base lubricant. It can also be interpreted

that the loos of material from JBL 10 is almost similar with base lubricant and this loos of material is increasing with increasing biolubricant percentages.

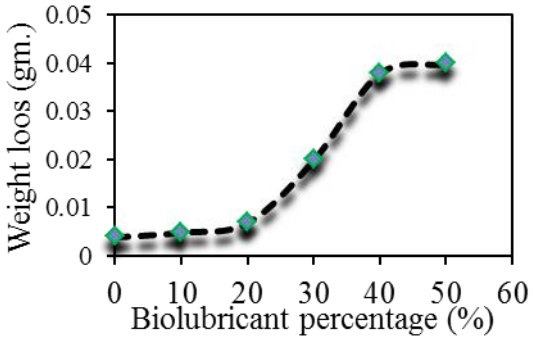

Fig.4. loos of material form the pin for various biolubricant percentages

3.2 Coefficient of Friction

Fig.5 shows the friction coefficient plotted against the sliding time for various Jatropha oil biolubricants. The results of the figure depict that the lubricant regime that occurred during the experiment were the boundary lubrication with the value of friction coefficient for boundary lubricant in the range of 0.001 to 0.2 except for 50% of Jatropha oil biolubricant. For JBL 0, it can be seen that the coefficient of friction is highest at the beginning and then it fell down rapidly and became least with compared to all tested samples after half of the operation time. The biolubricant percentage from 10 to 40% showed likely to be similar coefficient of friction (μ) which is almost 0.15. Whereas, the 50 % added Jatropha oil showed the coefficient of friction value of ~ 0.225 throughout the operation time. The fatty acid component of biolubricants formed multi and mono layer on the surface of the rubbing zone and make stable film to prevent the contact between the surfaces.

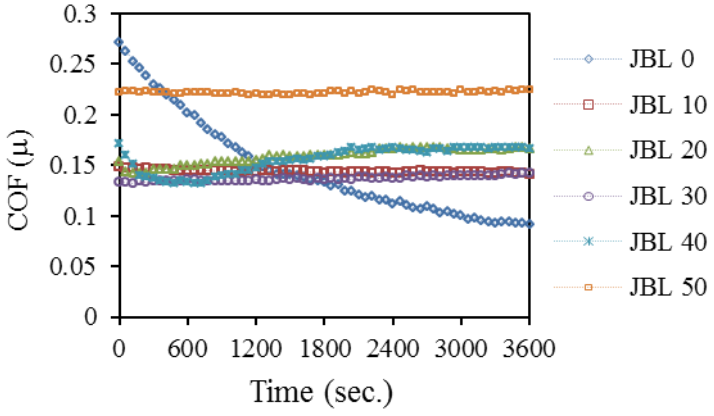

Fig. 5. The Coefficient of friction as a function of sliding time for various Jatropha oil biolubricants

3.3 Lubricants Temperature

Fig.6 shows the relationship of the averages oil temperature of varies percentage of Jatropha oil biolubricants with the sliding time. The rise of temperature during the running hour (1 h) for JBL 10 is least while the highest change is occurred for JBL 40 which is 11.77°c and 25.49°C respectively. The temperature rises of other samples are of 12.8°C, 18.65°C and

13. 66°C for 20% 30% and 50% Jatropha oil added biolubricants respectively. The results of the Fig. 6 show that the JBL 10 has the highest potentiality to retain its property without much changing its temperature. From the figure it can also be interpreted that up to 30 minutes rate of change of temperature is high while the changing rate is low for second half of the operation time. It can be explained that during second half of the operation time heat produced in the lubricant due friction and the heat dissipated to the outside is nearly equilibrium.

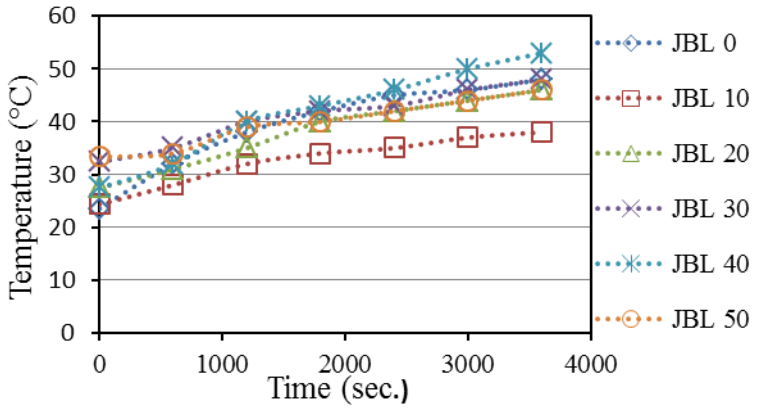

Fig. 6 The Lubricant Temperature as a function of sliding time for various Jatropha oil biolubricants

3.4 Viscosity

Viscosity is the measure of resistance to flow [18]. Table 2 shows the viscosity grade requirement for the lubricants set by International standard organization (ISO), while Fig. 7 shows the viscosity of tested different biolubricant samples. The comparison of the results of the Fig.7 with that of ISO grade illustrates that in case of 40°C, the biolubricants JBL 40 and JBL 50 did not meet the ISO VG100 requirement. On the other hand all other biolubricants meet the entire ISO grade requirement as well. It can also be noted that the viscosity of biolubricants are much higher than standard requirements

Table 2 ISO Viscosity grade requirement [19]

Kinematic viscosity	ISO VG32	ISO VG46	ISO VG68	ISO VG100
@ 40°C	>28.8	>41.4	>61.4	>90
@ 100°C	>4.1	>4.1	>4.1	>4.1

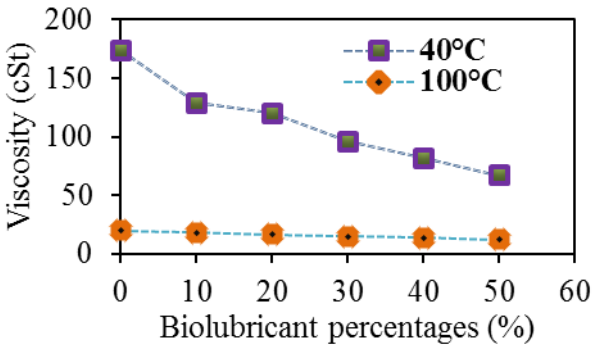

Fig. 7 The viscosity of various percentages of biolubricants at 40°C and 100°C

3.5 Elemental analysis

The aim of the elemental analysis by using Multi Element Oil Analyzer (MOA) is to determine the kinds and amount of metal contain in the lubricating oil. Table 3 shows the elemental analysis of tested lubricant sample by using MOA before and after the test. From the Table 3, it can be noticed that the base lubricant contains higher Silver (Ag), Zinc (Zn), Phosphorus (P), Magnesium (Mg) and Boron (B) with in high percentage compared to other element while, in pure Jatropha oil, Calcium (Ca) and Silicon (Si) are the higher element compared with other element. Some of the elements are used as additive in the lubricant to ameliorate the lubricants tribological properties. From the results, increasing number of iron (Fe) and aluminum (Al) molecules are observed with increasing percentages of Jatropha oil in the base lubricants. The source of Fe and Al are mainly cast iron plate and aluminum plate. Due to lower hardness of the aluminum pin the extraction of aluminum molecule form the pin is much higher than cast iron plate. The changes of other elements were observed before and after the test. It is clear from the elemental analysis that, most of elements were decreased after the test by oxidizing and the chemical interaction among the elements presents in the lubricants.

Table 3 Elemental analysis of tested lubricant sample

Parameters	Types of Lubricant												
	JBL 0		JBL 10		JBL 20		JBL 30		JBL 40		JBL 50		Jatropha oil
Test	Before	After	Before	After	Before	After	Before	After	Before	After	Before	After	
Iron (Fe)	0.00	2.00	1.00	2.00	1.00	3.00	1.00	3.00	1.00	6.00	2.00	6.00	2
Aluminium (Al)	0.00	15.00	0.00	81.00	0.00	188.00	0.00	205	0.00	211.0	0.00	76.00	0
Copper (Cu)	0	1.00	0.00	3.00	1.00	1.00	1.00	1.00	1.00	7.00	2.00	5.00	3
Lead (Pb)	3	4.00	4.00	5.00	2.00	4.00	3.00	4.00	3.00	3.00	3.00	2.00	0
Tin (Sn)	0.00	0.00	0.00	0.00	0.00	0.00	0.00	0.00	1.00	0.00	2.00	2.00	4.5
Nickel (Ni)	2.00	2.00	3.00	3.00	1.00	3.00	3.00	3.00	3.00	3.00	2.00	2.00	1.5
Titanium (Ti)	0.00	0.00	1.00	1.00	0.00	1.00	0.00	1.00	0.00	0.00	1.00	1.00	1
Silver (Ag)	108	103	0.00	0.00	0.00	0.00	0.00	0.00	0.00	0.00	0.00	0.00	0
Molybdenum (Mo)	3.00	3.0	4.00	6.00	2.00	3.00	4.00	3.00	4.00	6.00	3.00	4.00	1.5
Zinc (Zn)	1000	771	903	716	1000	829.0	911.0	851.0	942.00	900.0	946.00	832.00	1
Phosphorus (P)	500.00	428	471	441	462.00	440.0	435.00	408.0	387.00	394.0	348.00	294.00	45
Calcium (Ca)	18.00	17.00	21.00	29.00	23.00	21.0	28.00	27.0	35.00	33.00	37.00	30.00	40
Magnesium (Mg)	748.00	637.0	572.	616.00	557.00	435.0	503.00	527.0	508.00	483.0	409.00	211.00	27
Silicon (Si)	5.00	4.00	6.00	10.00	6.00	15.0	8.00	12.0	9.00	13.0	14.00	7.00	16
Sodium (Na)	2.00	1.00	2.00	5.00	2.00	2.0	3.00	4.00	5.00	4.00	3.00	4.00	4
Boron (B)	60.00	54.00	52.00	58.00	52.00	28.0	52.00	32.0	44.00	44.0	40.00	21.00	0.5
Vanadium (V)	0.00	1.00	0.00	1.00	0.00	0.00	1.00	0.00	1.00	0.00	1.00	1.00	1

3.6 Surface Texture analysis

There are various types of wear in the mechanical system, such that abrasive wear, adhesive wear, fatigue wear and corrosive wear. Since the lubricant regime occurred in this experiment was boundary lubrication thereby, abrasive wear, adhesive wear, fatigue wear and corrosive wear were observed in to the rubbing zone. All these wears mechanisms found in this experiments but the mostly the wear phenomenon were abrasive and adhesive wear. This is because of an existence of straight grooves in the direction of the sliding direction. These grooves exist because the asperities on the hard surface (disc) touched the soft surface (pins) and hade a close relationship with the thickness of lubrication film. The optical images of the tested cast iron plate using various types of biolubricants are shown in Fig. 8. Referring to the Fig. 8, it is found that the wear increases with increasing percentage of Jatropha oil in the biolubricants. Reduction of lubricant film thickness leads to the surfaces to come closer to each other and cause higher wear.

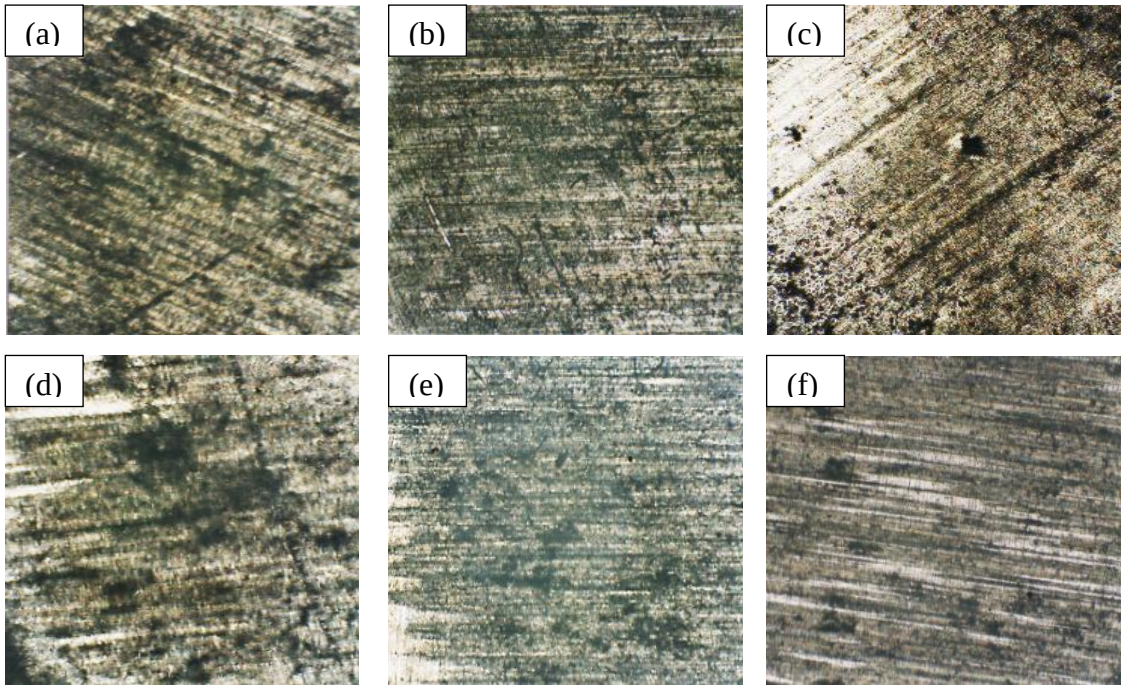

Fig.8 Optical image of the surface of the cast iron plate for different biolubricants (magnification 30 ×): (a): JBL 0, (b): JBL10, (c): JBL 20, (d): JBL 30, (e): JBL 40, (f): JBL 50

Acknowledgment

The authors would like to acknowledge the Department of Mechanical Engineering, University of Malaya, Ministry of Higher Education (MOHE) of Malaysia for HIR grant (Grant No. UM.C/HIR/MOHE/ENG/07) and ERGS grant no ER022-2011A which made this study possible.

Conclusion

Based on the experimental study the following conclusion can be drawn:

1. The rates of wear for various percentage of biolubricant were different. Moreover the wear rate for 10% Jatropha added biolubricants were almost identical with base lubricant.

2. Lower the resistance to wear, higher coefficient of friction.

3. At the beginning of the test rate of wear as well as rise in temperature were high. With respect to wear rate and rise in temperature during entire operation time, the JBL 10 biolubricant showed best performance in terms of its ability to withstand its properties.

4. From the elemental analysis of the biolubricants, it is found, Iron and Aluminium were increased after the test due to the loos of material from the pin and the disc while, some element like Phosphorus, Calcium and Magnesium were decreased by oxidizing and due to other chemical interaction.

5. In terms of viscosity, almost all biolubricants met the ISO viscosity grade requirement whereas, 40% and 50% addition of Jatropha oil do not meet the ISO VG 100 requirement at 40°C.

According to the experimental result, it can be recommended that the addition of 10% Jatropha oil in the base lubricant is the optimum for the automotive application as it showed best overall performance in terms of wear, coefficient of friction, viscosity, rise in temperature etc.

References

[1] Salih N, Salimon J, Yousif E. Synthetic biolubricant basestocks based on environmentally friendly raw materials. Journal of King Saud University – Science 2011.

[2] Adhvaryu A, Liu Z, Erhan S. Synthesis of novel alkoxylated triacylglycerols and their lubricant base oil properties. Industrial Crops and Products 2005; 21:113-119.

[3] Shahabuddin M, Masjuki HH, Kalam MA *et al.* Effect of Additive on Performance of C.I. Engine Fuelled with Bio Diesel. Energy Procedia 2012; 14:1624-1629.

[4] Siniawski MT, Saniei N, Adhikari B, Doezema LA. Influence of fatty acid composition on the tribological performance of two vegetable-based lubricants. Journal of Synthetic Lubrication 2007; 24:101-110.

[5] Salunkhe DK. World oilseeds: chemistry, technology, and utilization. 1992.

[6] Hwang HS, Erhan SZ. Lubricant base stocks from modified soybean oil. AOCS Press: Champaign, IL; 2002.

[7] Ing TC, Rafiq AKM, Syahrullail S. Friction Characteristic of Jatropha Oil using Fourball Tribotester. In: Regional Tribology Conference - RTC2011. Langkawi, Kedah, Malaysia: 2011.

[8] M. Shahabuddin, M. A. Kalam, H. H. Masjuki, M. Mofijur. Tribological characteristics of amine phosphate and octylated/butylated diphenylamine additives infused biolubricant. Energy Education Science and Technology Part A: Energy Science and Research 2012; 30:89-102.

[9] Totten G.E., Westbrook S.R, Shah R.J. Fuels and Lubricants Handbook: Technology,Properties, Performance, and Testing. 2003. 885–909. p.

[10] Liaquat AM, Masjuki HH, Kalam MA *et al.* Application of blend fuels in a diesel engine. Energy Procedia 2012; 14:1124-1133.

[11] Jayadas N, Nair KP. Coconut oil as base oil for industrial lubricants--evaluation and modification of thermal, oxidative and low temperature properties. Tribology international 2006; 39:873-878.

[12] Fox N, Stachowiak G. Vegetable oil-based lubricants—a review of oxidation. Tribology international 2007; 40:1035-1046.

[13] Waleska C, David EW, Kraipat C, Joseph MP. The effect of chemical structure of base fluids on antiwear effectiveness of additives. Tribol. Int. 2005; 38:321–6.

[14] Ponnekanti N, Kaul S. Development of ecofriendly/biodegradable lubricants: An overview. 2012.

[15] Mofijur M, Masjuki HH, Kalam MA *et al.* Palm Oil Methyl Ester and Its Emulsions Effect on Lubricant Performance and Engine Components Wear. Energy Procedia 2012; 14:1748-1753.

[16] Quinchia L, Delgado M, Valencia C *et al.* Viscosity modification of different vegetable oils with EVA copolymer for lubricant applications. Industrial Crops and Products 2010; 32:607-612.

[17] Quinchia L, Delgado M, Valencia C *et al.* Viscosity modification of high-oleic sunflower oil with polymeric additives for the design of new biolubricant formulations. Environmental science & technology 2009; 43:2060-2065.

[18] Shahabuddin M, Kalam MA, Masjuki HH *et al.* An experimental investigation into biodiesel stability by means of oxidation and property determination. Energy 2012.

[19] Rudnick LR. Automotives Gear Lubricants, Synthetics, mineral oils, and bio-based lubricants: chemistry and technology. Taylor and Francis, Florida; 2006.

Available online at www.sciencedirect.com

SciVerse ScienceDirect

Procedia Engineering 00 (2012) 000–000

Procedia Engineering

www.elsevier.com/locate/procedia

5th BSME International Conference on Thermal Engineering

Effect of operating conditions on the performance of adsorption solar cooling run by solar collectors

Rifat Ara Rouf[a], K. C. Amanul Alam[b], M. A. Hakim Khan[c] *

[a]School of Engineering and Computer Science, Independent University, Bangladesh, Dhaka, 1229, Bangladesh,
[b]Department of Electronics and Communication Engineering, East-West University, Dhaka, 1212, Bangladesh,
[c]Department of Mathematics, Bangladesh University of Engineering and Technology, Dhaka, 1000, Bangladesh.

Abstract

Adsorption solar cooling appears to have prospect in the tropical countries. The present study investigates the effect of operating conditions on the performance of solar powered adsorption chiller for the climatic condition of Dhaka (Latitude $23^{\circ}46'$ N, Longitude $90^{\circ}23'$ E). A set of mathematical equations has been utilized to investigate the performance of the system numerically. Based on the solar radiation data, it is seen that at least 13 collectors (each of area $2.42\,m^2$) are essential to achieve the required heat source temperature in the hot and humid months. It appeared during the investigation that the unit provides the cooling capacity around 10 kW at noon with base run conditions, while the system provide the solar COP around 0.35. As the cycle time has a major effect on heat source temperature as well as on system performance, it is observed that there is an optimum cycle time for the collector size. Also, the performance of the chiller can be improved by controlling the chilled water flow rates. Therefore, it may be concluded that the collector size may be reduced by setting the optimum cycle time and the chilled water flow rate.

Keywords: Adsorption; Solar heat; Renewable energy; Air-conditioning.

Nomenclature

A	Area (m^2)
c_p	specific heat (J/kgK)
I	solar radiation (W/m^2)
$\dot{m}$	mass flow rate (kg/s)
t	time (S)
T	temperature (K)
Subscripts	
chill	chilled water
f	heat transfer fluid
n	number of collector

* Corresponding author. Tel.: 880-2-01711407417; fax: 880-2-840-1919.
E-mail address: rifatar@iub.edu.bd

1. Introduction

Increasing population, global warming and power crisis are the burning issues of the developing countries of the twenty first century. Most of the space cooling or air-conditioning technologies use conventional energy sources as well as use global warming gases. It is getting essential to look for alternative energy sources and environmentally benign gases for this system. Nowadays, adsorption refrigeration and air conditioning cycles have drawn considerable attention due to its ability to be driven by low temperature heat source and for the environmental aspects as it uses environment friendly refrigerants. The advantage and development of adsorption cycle is widely studied by Meunier [1]. Extensive studies about adsorption refrigeration and air conditioning cycles have been conducted by various researchers for the development of adsorption technology. The studies mainly focused on either to enhance COP value of the system, such as, advanced cascaded cycle Meunier [2] and thermal wave cycle Shelton et al [3] or to improve system cooling capacity, such as, mass recovery cycle Wang [4] and Akahira et al. [5] and reheat two-stage cycle Alam et al. [6]. Advanced cycle could be also designed for better utilization of heat source, such as multi-bed system [7] and for utilization of low temperature heat source, such as, three-stage cycle [8] and two-stage cycle [9].

As adsorption cooling system can be driven by low heat source temperature, it could be effective to utilize solar heat. In this context, Sakuda and Suzuki [10] studied the simultaneous transport of heat and adsorbate in closed type adsorption cooling system utilizing solar heat in which authors proposed a lumped parameter model to predict the performances of the system. Solar ice making with adsorption technology has been also extensively studied by Leite and Daguenet [11] and Boubarkri [12]. Yang and Sumanthy [13] exploited lumped parameter model for two beds adsorption cycle driven by solar heat where flat plate collector is used. Clausse et al. [14], considered the models of whole units of a residential air conditioning sytem to investigate the performances of the system for the climatic condition of Orly, France. Recently, Alam et al. [15] studied the silica-gel water adsorption cooling cycle with direct coupling of solar collector under the climatic condition of Tokyo.

A tropical country like Bangladesh has prospect in utilizing solar energy as a driving source for adsorption refrigeration and air conditioning system. In preservation of medicine and food at the rural and remote places, solar heat driven adsorption refrigeration cycle could play a major roll for Bangladesh. From this point of view, Rifat et al. [16] studied adsorption cooling system for the climatic condition of Dhaka. The present study investigates the effect of some important operating system on the performances of the solar heat driven adsorption cycle.

1.1.Principal and operational process of the system

A two-bed conventional adsorption cooling cycle driven by solar heat has been considered. Silica gel-water pair as adsorbent/adsorbate and basic adsorption cooling cycle has been considered in the present study. There are four thermodynamic steps in the cycle. Two adsorption beds, an evaporator, a condenser, 13 solar collectors and a cooling tower are connected in the system. The schematic of the adsorption cooling with solar collector panel is presented in Fig 1. The adsorber (A1/A2) alternatively connected to the solar collector to heat up the bed during preheating and desorption-condensation process and to the cooling tower to cool down the bed during pre-cooling and adsorption-evaporation process. The cooling source temperature is considered to be ambient temperature. The heat transfer fluid from the solar collector goes to the desorber and returns the collector to gain heat from the collector. The valve between adsorber and evaporator and the valve between desorber and condenser are closed during pre-cooling/pre-heating period. While these are open during adsorption-evaporation and desorption-condensation process. Logical programming language FORTRAN with Compaq Visual Fortran compiler has been exploited to obtain the numerical solution of the proposed model.

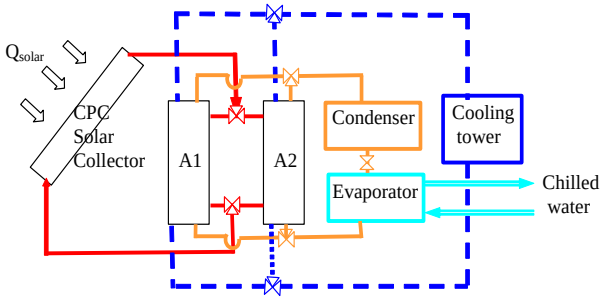

Fig. 1. Schematic of the solar driven adsorption space cooling system.

1.2.Mathematical model

It is assumed that the temperature, pressure and concentration throughout the adsorbent bed are uniform. The mathematical model is same as Alam et al [15].

The cyclic average cooling capacity is calculated by the equation

$$CACC = \dot{m}_{chill} C_{chill,f} \left(\int_{beginofcycletime}^{endofcycletime} \left(T_{chill,in} - T_{chill,out} \right) dt \right) \Big/ t_{cycle} \tag{1}$$

The cycle *COP* (coefficient of performance) and solar *COP* in a cycle (COP_{sc}) are calculated respectively by the equations

$$COP_{cycle} = \frac{\int_{beginofcycletime}^{endofcycletime} \dot{m}_{chill} C_{chill,f} \left(T_{chill,in} - T_{chill,out} \right) dt}{\int_{beginofcycletime}^{endofcycletime} \dot{m}_{f} C_{f} \left(T_{d,in} - T_{d,out} \right) dt} \tag{2}$$

$$COP_{sc} = \frac{\int_{beginofcycletime}^{endofcycletime} \dot{m}_{chill} C_{chill} \left(T_{chill,in} - T_{chill,out} \right) dt}{\int_{beginofcycletime}^{endofcycletime} n.A_{cr} I dt} \tag{3}$$

1.3. Simulation procedure

Measured monthly maximum radiation data for Dhaka (Latitude $23^{\circ}46'$ N, Longitude $90^{\circ}23'$E) has been used. This data is supported by the Renewable Energy Research Center (RERC), University of Dhaka. Results are generated based on solar data of Dhaka in the month of April. Chiller configurations are same as Saha et al. [18] and collector data are same as Alam et al. [15]. During April in Dhaka, the sunrise time is at 5.5h and sun set at 18.5h, whereas maximum temperature is 34°C and minimum temperature is 24°C. The maximum solar radiation in this month is about 988 W/m^2 . The detail design and operating conditions input data are given in Rifat et al. [16], where the prospect of solar adsorption cooling has been studied for the climatic condition of a tropical place Dhaka.

Implicit finite difference approximation method is applied to solve the set of differential equations. The tolerance for all the convergence criteria is 10^{-4}. The program runs for consecutive several days (as it is set). After a few days the system appears to its steady state. In this paper all results are presented for the day when the system appeared at its' steady state, i.e. all output appeared to be identical for the consecutive days. The detail description of simulation is available in Alam et al. [15].

2. Result and discussion

Thirteen collectors, each of area 2.415m^2, has been taken into consideration for the present analysis. The number of collectors has been decided based on Rifat et al. [16], where a case study had been conducted to examine the performance of solar heat driven adsorption cooling unit based on the climatic condition of Dhaka. According to this study, for the month of April, 13 collectors with optimum cycle time 1000s are sufficient to run the solar cooling unit. However, later Rifat et al. [17] while investigating the prospect of the said solar unit, had concluded that the optimum cycle time and performance varies with various seasons of the year. The program is allowed to run with different cooling water inlet temperature and taking different amount of supply of chilled water to the evaporator. The rest of the operating conditions are same as Rifat et al. [16].

At first, the number of collectors and cycle time were determined for base run conditions to achieve driving source temperature level which is around 80°C for silica-gel water pair [18-19]. Then the investigation was extended to check the

performances of the system of the present study. Figure 2 presents the temperature histories of collector outlet and bed for cycle time 1000sec, the collector outlet temperature reaches 87°C while the bed temperature reaches 85°C. Rifat et al. [16] showed that when the cycle time is reduced from 1000sec the bed temperature is below 75°C. Therefore, 1000sec, the optimum cycle time is taken into consideration for running the chiller when 13 collectors are in use. The temperature of cooling source is considered as ambient temperature that is 31°C and chilled water inlet temperature is 14°C. The volumetric flow rate of chilled water to evaporator is 0.7 kg/sec.

Figure 3 depicts the effect of cooling source temperature on the performances of the chiller. For the time being it appears that the cooling capacity increases when the cooling source temperature decreases. The reason of the increase in the cooling capacity is due to the increase of the adsorption capacity of silica gel bed as the temperature lift (difference between hot and cooling source temperature) increases. The same trend has been observed for cycle COP and Solar COP in a cycle. However, the coefficient of performance of the chiller increases until late afternoon and suddenly start to decline and this trend for 28°C cooling source temperature is higher than the other cases. It happens due to higher cooling capacity in late afternoon comparing the heat input at that time. The chiller is capable in producing 10 kW cooling at noon when the cooling source temperature is considered as 31°C.

The effect of chilled water flow rates on the performance of the chiller are shown in Fig 4. This figure shows that the performances (CACC, COPcyle and COPsc) of the chiller are proportional to the chilled water mass flow rates at least until 5pm. However, opposite trends are shown after 5pm. If we notice Equations (1)-(3), it is seen that the performances are directly proportional to chilled water mass flow rates as well as to the temperature difference between chilled water inlet and outlet. At the same time, chilled water outlet temperature is strongly influenced by the chilled water flow rates. This effect is visible in Fig 5.

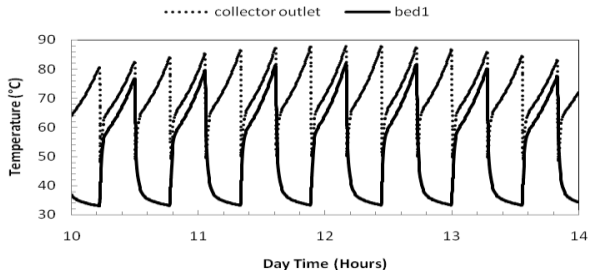

Fig. 2. Temperature histories of collector outlet and bed for 13 collector cycle time 1000s

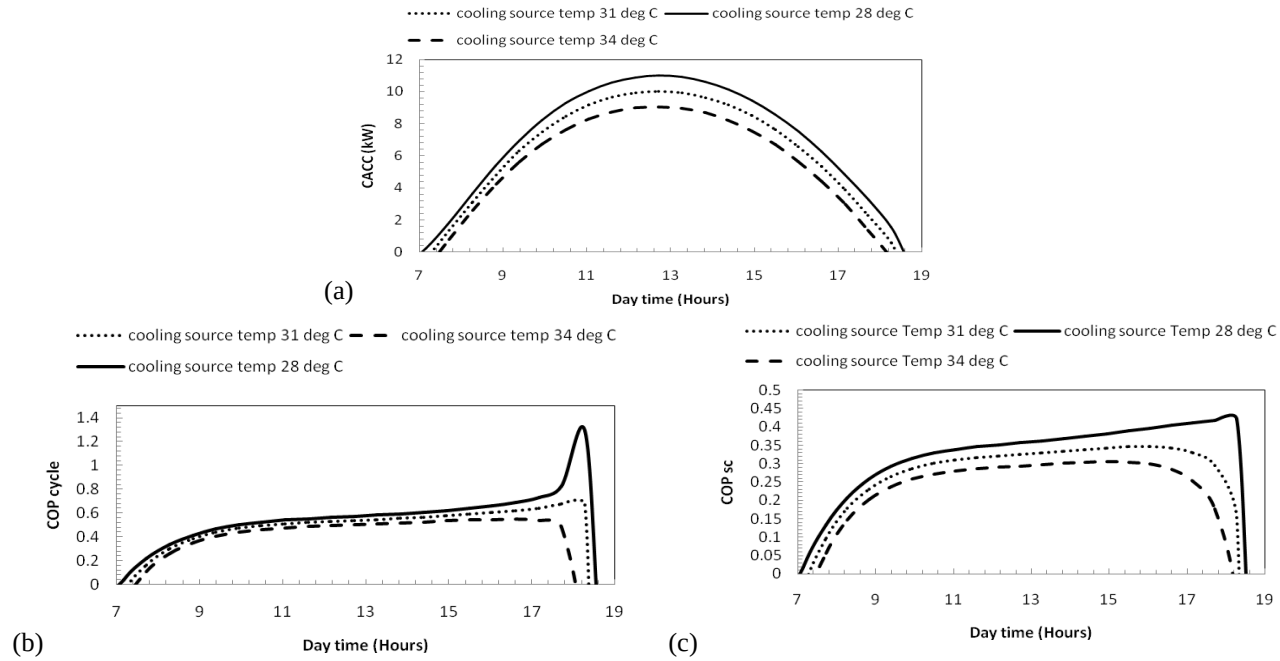

Fig . 3. Performance of the chiller for different temperature cooling water supply to the adsorber (a) cyclic average cooling capacity, (b) COP cycle and (c) COP sc

Chilled water outlet temperature histories of 13 collectors with different volumetric flow rate have been depicted in Fig 5. It is seen that the lower the flow rates of chilled water the lower temperature of chilled water outlet. Chilled water outlet is importrant for the end user as outlet chilled water is utilized for space cooling. It is seen that Cooling capacity and COP are increasing with the increase of chilled water mass flow rate. But at the same time, increase in chilled water mass flow rate causes increase in chilled water outlet tempertaure which may cause uncomfort to enduser. Therefore, it is important to select appropriate chilled water flow rate so that the system can provide better performance and appropriate chilled water outlet temperature.

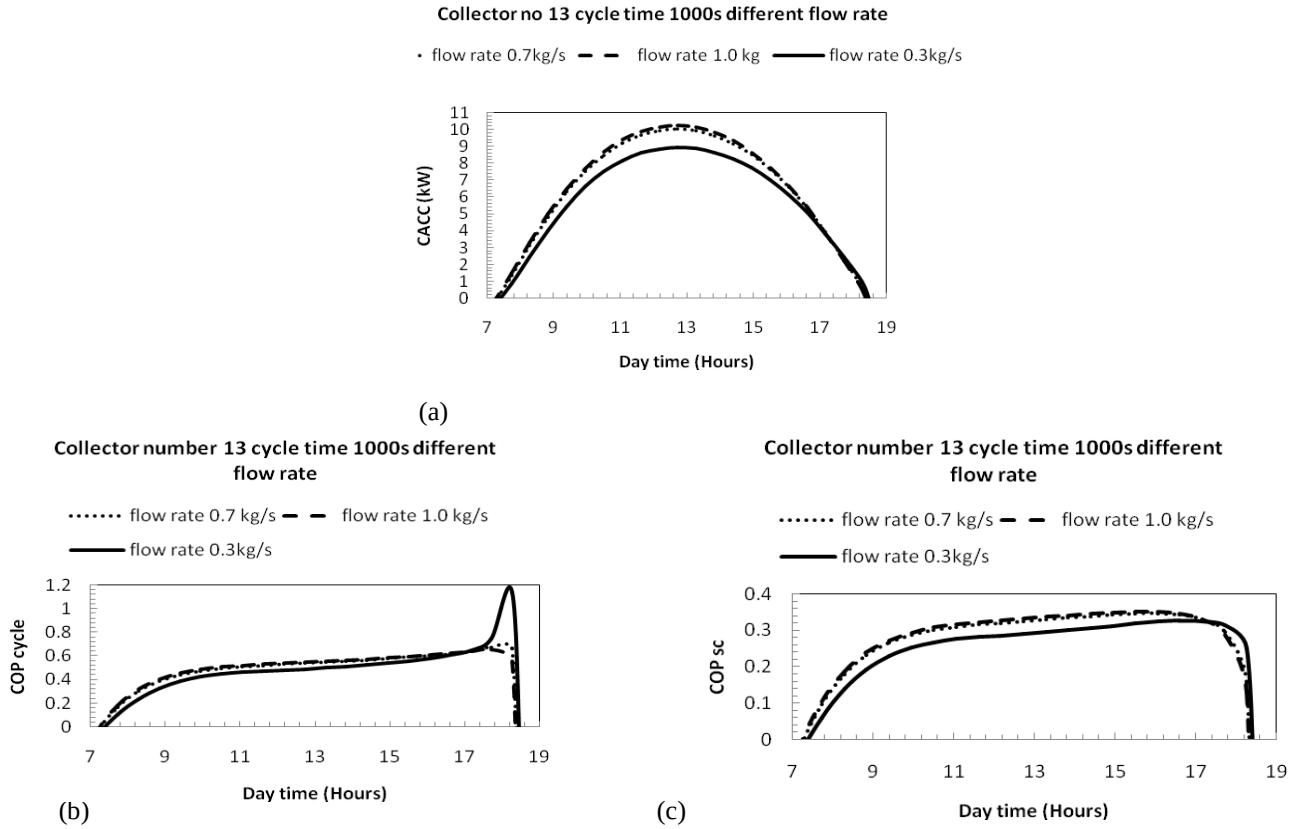

Fig. 4. Performance of the chiller with 13 collectors cycle time 1000s with different chilled water flow rate (a) CACC, (b) COP cycle and (c) COP sc

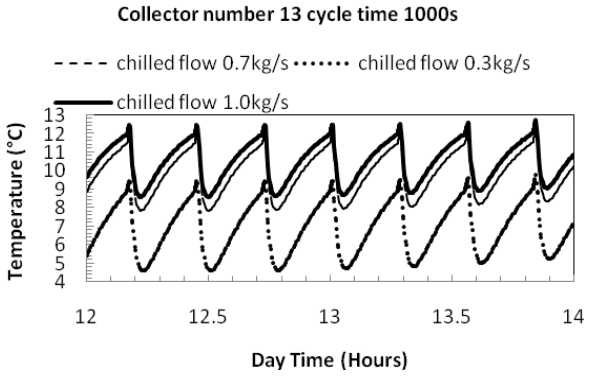

Fig. 5. Chilled water outlet temperature for 13 collectors different chilled water flow rates

3. Conclusion

An analytical investigation has been conducted to examine the effect of operating condition on solar driven adsorption air-conditioning system for the climatic condition of Dhaka. 13 collectors each of area 2.415 m^2 with optimum cycle time 1000sec has been studied with different temperature of cooling source and chilled water flow rates for base run conditions.

Based on the investigation the following conclusions can be drawn.

- Cooling capacity and COP increases with the decrease of cooling source temperature.
- COP of the chiller can be improved by increasing the flow of the chilled water to the evaporator, at the same time it causes increase in the temperature of chilled water outlet.
- Chilled water outlet temperature could be controlled by controlling the flow rates of chilled water.
- At least 31°C cooling water and 14°C chilled water flow of 1 kg/sec is needed to ensure 10kW cooling capacity, 0.6 cycle COP and 0.35 solar COP for 13 collectors with optimum cycle time 1000sec in base run condition at noon.

Acknowledgement

The author expresses her gratitude to Prof. Dr. Saiful Huque, Dr. Himangshu Ranjan Ghosh of RERC and Mr. Md. Abdur Rahman Khan of BMD for their assistance in data collection. The author also thanks her director of school Prof. Dr. Md Anwer for his time and advice providing language help. She cannot thank less to her colleague Mr. Khaled Mahmud for his assistance in formatting the manuscript.

References

[1] Meunier, F., 1998. Solid Sorption Heat Powered Cycles for Cooling and Heat Pump Applications. Applied Thermal Engineering 18, p. 714.
[2] Meunier, F., 1986.Theoretical Performance of Solid Adsorbent Cascading Cycles using Zeolite-water and Active Carbon-methanol Pair; Four Cases studies. Heat Recovery CHP System 6(6), p. 491.
[3] Shelton, S.,V., Wepfer, J., W., Miles, D., J., 1990. Ramp Wave Analysis of the Solid/Vapor Heat Pump. ASME Journal of Energy Resources Technology 112, p. 69.
[4] Wang, R., Z., 2001. Performance Improvement of Adsorption Cooling by Heat and Mass Recovery Operation, International Journal of Refrigeration 24, p. 602.
[5] Akahira, A., Alam, K., C., A., Hamamoto, Y., Akisawa, A., Kashiwagi, T., 2005. Experimental Investigation of Mass Recovery Adsorption Refrigeration Cycle. International Journal of Refrigeration 28, p. 565.
[6] Alam, K., C., A., Khan, M., Z., I., Uyun, A., S., Hamamoto, Y., Akisawa, A., and Kashiwagi, T., 2007. Experimental Study of a Low Temperature Heat Driven Re-heat Two-stage Adsorption Chiller. Applied Thermal Engineering 27, p. 1686.
[7] Chua, H., T., Ng, K., C., Malek, A., Kashiwagi, T., Akisawa, A., Saha, B., B., 2001. Multi-bed Regenerative Adsorption Chiller—Improving the Utilization of Waste Heat and Reducing the Chilled Water outlet Temperature Fluctuation. International Journal of Refrigeration 24, p. 124.
[8] Saha, B., B., Boelman, E., C., Kashiwagi, T., 1995. Computational Analysis of an Advanced Adsorption Refrigeration Cycle. Energy 20, p. 983.
[9] Alam, K., C., A., Saha, B., B., Akisawa, A., and Kashiwagi, T., 2004. Influence of Design and Operating Conditions on the System Performances of a Two-stage Adsorption Chiller. Chemical Engineering Communications 191, p. 981.
[10] Sakoda, A., Suzuki, A., M., 1986. Simultaneous Transport of Heat and Adsorbate in Closed Type Adsorption Cooling System Utilizing Solar Heat.Journal of Solar Energy Engineering 108, p. 239.
[11] Leite, A., P., F., Daguenet, M., 2000. Performance of a New Solid Adsorption Ice Maker with Solar Energy Regeneration. Energy Conversion and Management 41, p. 1625.
[12] Boubakri, A., 2003. A New Conception of an Adsorptive Solar Powered Ice Maker. Renewable Energy 28, p. 831.
[13] Yong, L., Sumathy, K., 2004. Modeling and Simulation of a Solar Powered Two Bed Adsorption Air Conditioning System. Energy Conversion and Managemen. 45, p. 2761.
[14] Clausse, M., Alam, K., C., A., Meunier, F., 2008. Residential Air Conditioning and Heating by means of Enhanced Solar Collectors Coupled to an Adsorption System. Solar Energy 82 (10), p. 885.
[15] Alam, K., C., A, Saha, B., B., and Akisawa, A., 2011. Adsorption Cooling Driven by Solar Collector: a Case Study for Tokyo Solar Data. Applied Thermal Engineering, in press.
[16] Rouf, R., A, Alam, K., C., A., Khan, M., A., H., Ashrafee, T., Anwer, M., 2012. Solar Adsorption Cooling: a Case Study on the Climatic Condition of Dhaka. Academy Publishers Journal of Computers, accepted.
[17] Rouf, R., A., Alam, K., C., A., Khan, M., A., H., Ashrafee, T., 2011. "Prospect of solar cooling based on the climatic condition of Dhaka," Proceedings of 9th International Conference on Mechanical Engineering, paper #RE-14.
[18] Saha, B., B., Boelman, E., C., Kashiwagi, T., 1995. Computer Simulation of a Silica gel- water Adsorption Refrigeration Cycle – the Influence of Operating Conditions on Cooling Output and COP. ASHREA Transactions 101 (2), p. 348.
[19] Chua, H., T., Ng, K., C., Malek, A., Kashiwagi, T., Akisawa, A., Saha, B., B., 1999. Modeling the Performance of Two bed, Silica gel-water Adsorption Chillers. International Journal of Refrigeration 22, p. 194.

Available online at www.sciencedirect.com

SciVerse ScienceDirect

Procedia Engineering 00 (2012) 000–000

Procedia Engineering

www.elsevier.com/locate/procedia

5th BSME International Conference on Thermal Engineering

Linear Fresnel Mirror Solar Concentrator with Tracking

P.K. Sen*, Ashutosh K,, Bhuwanesh K., Z. Engineer, S. Hegde, P.V. Sen, P. Davies[a]

Dept. of Applied Mechanics, Indian Institute of Technology Delhi, New Delhi 110016, India
[a]Dept. of Engineering & Applied Sciences, Aston University, Address, Aston Triangle, Birmingham, B4 7ET, UK

Abstract

Solar energy is the most abundant, widely distributed and clean renewable energy resource. Since the insolation intensity is only in the range of 0.5 - 1.0 kW/m^2, solar concentrators are required for attaining temperatures appropriate for medium and high temperature applications. The concentrated energy is transferred through an absorber to a thermal fluid such as air, water or other fluids for various uses. This paper describes design and development of a 'Linear Fresnel Mirror Solar Concentrator' (LFMSC) using long thin strips of mirrors to focus sunlight on to a fixed receiver located at a common focal line. Our LFMSC system comprises a reflector (concentrator), receiver (target) and an innovative solar tracking mechanism. Reflectors are mirror strips, mounted on tubes which are fixed to a base frame. The tubes can be rotated to align the strips to focus solar radiation on the receiver (target). The latter comprises a coated tube carrying water and covered by a glass plate. This is mounted at an elevation of few meters above the horizontal, parallel to the plane of the mirrors. The reflector is oriented along north-south axis. The most difficult task is tracking. This is achieved by single axis tracking using a four bar link mechanism. Thus tracking has been made simple and easy to operate. The LFMSC setup is used for generating steam for a variety of applications.

Keywords: linear fresnel mirror concentrator; line focusing.

Nomenclature

A_g	total ground area covered by the reflector
A_m	total mirror area
B	width of the mirror strip
I_b	total beam radiation
L	length of mirror strip
M_s	mass flow rate in the receiver
Q_a	energy absorbed by the receiver
Q_s	heat absorbed by the fluid in the receiver
ΔT	change in temperature
Greek symbols	
ϕ	fraction of ground covered by the mirrors
α	absorbance of the receiver
η_o	fraction of solar radiation focused on to the receiver

*Corresponding Author. Tel: +91-11-26591179; Fax: +91-11-26581119
E-mail address: pksen@am.iitd.ernet.in

1. Introduction

Though solar energy is widely distributed, it is dispersed and available only at the rate of 500-1000 W/m^2. Hence solar thermal concentrating collectors are required for capturing and directing the energy to a target for producing medium and high temperatures.

Solar collectors such as flat plate collectors are non-concentrating type which typically heat the target only up to 70 º C and are hence useful for only low temperature applications. By using a concentrating solar collector the sun's rays can be focused on a receiver to raise the temperature of the fluid flowing inside the receiver. Among concentrating collectors currently linear focusing cylindrical collectors and point focusing paraboloid collectors are quite popular [1].

Due to the ease of fabrication and handling, interest has been evoked on developing Linear Fresnel Mirror Solar Concentrator (LFMSC) [2-3]. In this paper we present our work on the design and development of LFMSC with a tracking device for small scale applications, especially for raising steam. The system comprises a Reflector (Concentrator), Receiver (Target) and Solar Tracking System which uses Four Bar Link Mechanism [4-5].

2. LFMSC Design and Fabrication

2.1. Reflector

The Linear Fresnel concentrator mirror reflector consists of a large number of long, narrow, flat mirrors strips mounted on tubes which are placed on a flat base frame. When the sun rays fall on Fresnel mirror strip they get reflected from the mirror to the receiver. The individual mirrors are oriented in such a manner that axially incident parallel rays of light intercepted by the concentrator are reflected to a common line focus on the receiver. The Fresnel reflector is shown schematically in Fig-1.

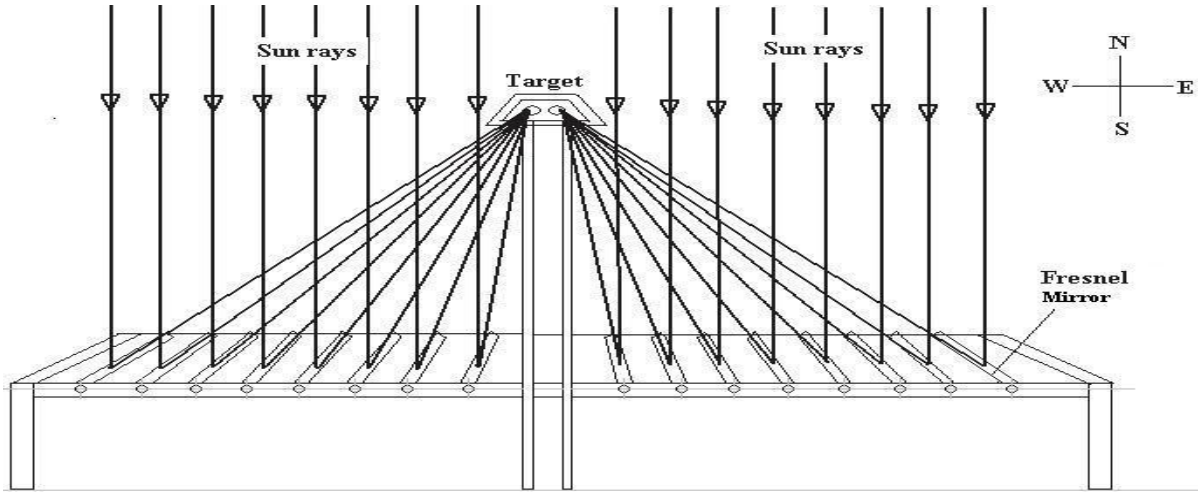

Fig. 1. Schematic diagram showing sun rays reflected to the Receiver by the Reflector.

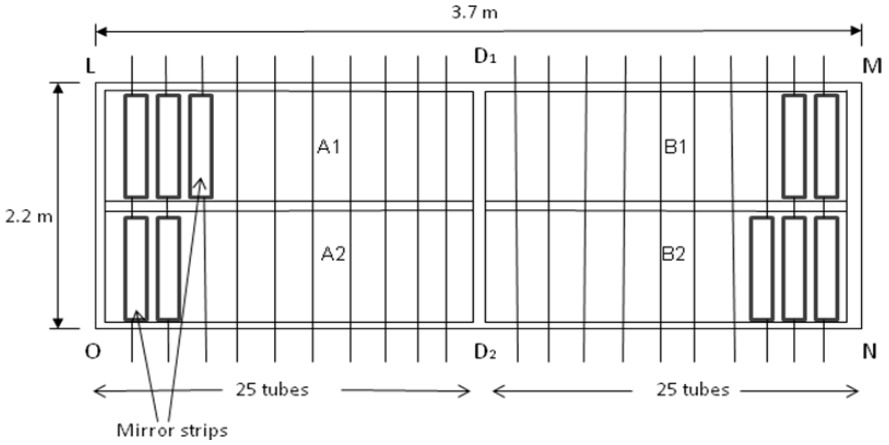

Fig. 2. Top view of Reflector

For each individual mirror the three specifying parameters, namely the clearance, tilt and width, were determined such that the concentrated radiation field produced is within the pre-specified location on the receiver giving a high concentration factor. In the experimental setup as shown in Fig. 2 the base frame LMNO is divided into two sections (A and B) in the middle by a support (divider D1-D2). 50 tubes of 2.2 m length were supported on the base frame through the carefully aligned drilled holes. Each section of the reflector is divided into two parts A1-A2 and B1-B2 as shown schematically. There are 25 mirror strips of 1 m length and width of 0.05 m, mounted on the tubes in each part. Thus a total number of 50 mirror strips are mounted on 25 tubes in section A and the same number in section B making a total of 100 mirror strips in the reflector.

2.2. Receiver (Target)

The receiver as shown in Fig. 3 consists of a pipe, which is folded and housed within a semi cylindrical (trapezoidal) outer casing with insulating packing of glass wool in the space between. To minimize radiation and convection losses it is covered by a glass plate at the bottom. The receiver is mounted at an elevation of few meters above the horizontal surface and parallel to the plane of the mirrors. It can be raised using pulleys and moved on rollers for shifting. Water as thermal fluid, enters from the inlet of the pipe which is fixed at the focal line of the reflector. It gets converted to steam by the time it reaches the outlet. A steam separator may be placed at the outlet to collect the steam and bypass the water back into the inlet loop.

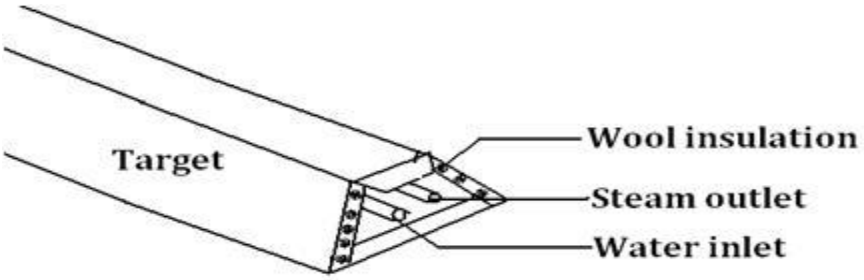

Fig. 3. Target with Internal parts

2.3. Tracking Mechanism

The orientation for the reflector setup has been chosen to be along the Horizontal North South axis rather than the polar axis. The latitude of Delhi being 30° and India being in the tropical zone and sufficiently close to the equator, we do not require polar configuration with declination angle, which is more advantageous farther away from the equator. Tracking was achieved by a four bar link mechanism in which the rotational motion provided to one tube gets transmitted to others also. In this way we can get equal deflection of all the tubes, making tracking easy. The tracking system shown in Fig. 4 uses the concept of parallelogram linkage as shown in Fig 5, which is a double crank mechanism. The motion transmitted to a single tube by a gear mechanism is transmitted equally to all the other tubes. The gears are rotated at the rate of 15^0 per hour by a small motor.

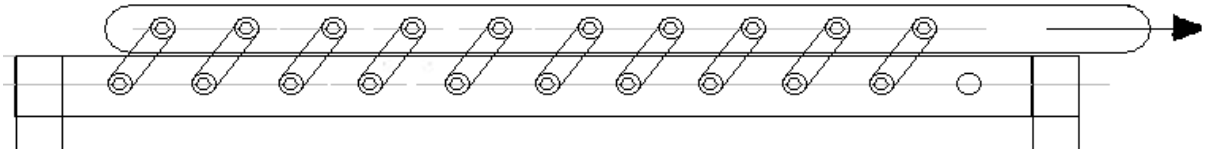

Fig. 4. Tube and Link Mechanism

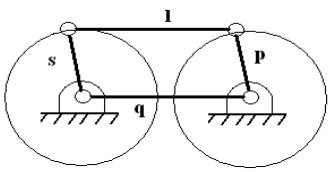

Fig. 5. Parallelogram Linkage between Tubes (s + l = p + q)

Steam Output Estimation

The mirror strips in the reflector system are to be laid such that both in winter season when sun is low and summer season, when sun is high, there is no shade of one mirror on the other mirror. Therefore the mirrors cover only a fraction of ground (ϕ), which is calculated as

$$\phi = \frac{A_m}{A_g} \quad (1)$$

Where, and A_m = (N x a_m) is the total mirror area, N being the number of mirrors, and a_m the area of single mirror strip. A_g is the total ground area covered by the reflector.
The energy absorbed by the receiver is given by the equation

$$Q_a = I_b \times A_m \times \eta_0 \times \alpha \quad (2)$$

Where, I_b is the total beam radiation on Am and η_o is the fraction of solar radiation focused on to the receiver, and α is the absorbance (The ratio of absorbed to incident radiation) of the receiver.

Experimental Model at IIT Delhi

In the current setup the number of mirror strips (N) are 100 (50 each side) of length (L) 1 m, width (B) 0.05 m, and thickness (T) 0.003 m.

Clearance (C) of 0.02 m is kept between mirrors to avoid blocking.

Thus the total reflector area (N xA_m) = (100×0.05×1) = 5 m^2 for 100 mirrors

Total ground area (A_g) covered is (100× (0.05+0.02) ×1) = 7 m^2

Fraction of ground covered $\phi = \frac{N \times A_m}{A_g} = \frac{5}{7} = 0.714$

Total energy absorbed by the receiver, Q_a is calculated by using Eqn. (2)

Solar radiation flux or the beam radiation available (I_b) is taken as, I_b = 700 W/m^2

Putting the values of A_m = 5 m^2, ηo x α = 0.5 in Eqn. (2)

Total energy absorbed Q_a = 1759 Watt (J/s) = 6300 KJ/hr

Q_s, the heat absorbed by the fluid in the receiver is given by

$$Q_s = M_s \text{ x } Cp \text{ x } \Delta T + M_s \text{ x } L = M_s \text{ x } [Cp\ \Delta T + L] \quad (3)$$

Where, M_s is the mass flow rate of water at inlet which is assumed to be fully converted to steam at outlet, Cp the specific heat of water, ΔT the temperature difference, and L the latent heat of vaporization of steam.

M_s can be calculated for different situations, by balancing the heat supplied to heat absorbed ($Q_a = Q_s$),

and putting the respective values of Cp = 4.178 KJ/Kg-k, L = 2257KJ/Kg and ΔT in Eqn. (2)

For example if steam is produced at atmospheric pressure from water at 30^0C, ΔT = 100 – 30 = 70,

M_s works out to be ≈2.5 Kg/hr

If the steam is needed above atmospheric pressure (say at 1.5 bar), ΔT = 120 – 30 = 90 as boiling point at 1.5 bar is approximately 120 ^{0}C. In this case M_s reduced to 2.4 Kg/hr

In case larger quantities of M_s is needed, a setup with a larger reflector area A_m has to be taken. In another set of experiments a system with A_m = 13 m^2 was setup. In this case for steam production M_s at 1.5 bar (i.e. at 120^0C) comes out to be 6.3 kg/hr.

Photographs of the experimental system fabricated are shown in Fig. 6(a-c).

Fig. 6. (a) fresnel concentrator setup, (b) another view of setup with tracking timer, (c) Tracking motor with gear box and linkage mechanism

Conclusion

Linear Fresnel Mirror Solar Concentrator system with mechanical tracking device was designed and fabricated. Four bar mechanism used here in is an innovation which makes the handling and operation facile. In this modular system using mirror strips as reflector the solar radiation is concentrated on the receiver at the focal line. The absorbed energy is carried by water as thermal the fluid to raise steam at desired pressure for small scale applications.
With a reflector area of 5 m^2, 2.4 kg/hr steam can be produced at 1.5 bar pressure, and with a reflector area of 13 m^2, 6.3 kg/hr steam can be produced at 1.5 bar.

Acknowledgement

Authors are thankful for the financial support under RC-UK DST, India funded project (EP/G021937/1). We are also thankful to Mr. D. C. Sharma and Mr. Sitaram (senior technicians at IIT Delhi), for their help during the course of the project.
We are thankful to Mr. Cyrus Engineer, Industrial Boilers Pvt. Ltd. for helpful discussions.

References

[1] Sukhatme, S. P., Nayak, J. K., 2008. Solar Energy, Principles of Thermal Collection and Storage, Tata McGraw-Hill Co., (2008).
[2] Mathur, S. S., Negi, B. S., Kandpal, T. C., 1991. Optical design and concentration characteristics of Linear Fresnel Reflector Solar Concentrator-I. Mirror Elements of varying width, Energy Conversion and Management Vol. 31, No. 3, pp. 205-219.
[3] Mathur, S. S., Negi, B. S., Kandpal, T. C., 1991. Optical design and concentration characteristics of Linear Fresnel Reflector Solar Concentrator-II, Mirror Elements of varying width, Energy Conversion and Management Vol. 31, No. 3, pp. 221-232.
[4] Kumar, Ashutosh, 2012. Studies on steam generation using Linear Fresnel Mirror Solar Concentrator with Tracking, M. Tech Thesis, Department of Applied Mechanics, IIT Delhi.
[5] Kumar, Bhuwanesh., 2012. Performance of Micro Scale Multi Effect Distillation system compatible with solar energy, M. Tech Thesis, Department of Applied Mechanics, IIT Delhi.

Available online at www.sciencedirect.com

SciVerse ScienceDirect

Procedia Engineering 00 (2012) 000–000

Procedia Engineering

www.elsevier.com/locate/procedia

5th BSME International Conference on Thermal Engineering

Optimisation of Bio-oil Extraction Process from Beauty Leaf (*Calophyllum inophyllum)* Oil Seed as a Second Generation Biodiesel Source

Jahirul M. I.[1]*, Brown J. R[1], Senadeera W[1], Ashwath N[2], Laing C[1], Leski-Taylor J[1], Rasul M. G.[2]

[1] *Science and Engineering Faculty, Queensland University of Technology (QUT), Brisbane, Australia*
[2] *Centre for Plant and Water Sciences (CPWS), Central Queensland University (CQU), Rockhampton, Australia*

Abstract

The Beauty Leaf tree *(Calophyllum inophyllum)* is a potential source of non-edible vegetable oil for producing future generation biodiesel because of its ability to grow in a wide range of climate conditions, easy cultivation, high fruit production rate, and the high oil content in the seed. This plant naturally occurs in the coastal areas of Queensland and the Northern Territory in Australia, and is also widespread in south-east Asia, India and Sri Lanka. Although Beauty Leaf is traditionally used as a source of timber and orientation plant, its potential as a source of second generation biodiesel is yet to be exploited. In this study, the extraction process from the Beauty Leaf oil seed has been optimised in terms of seed preparation, moisture content and oil extraction methods. The two methods that have been considered to extract oil from the seed kernel are mechanical oil extraction using an electric powered screw press, and chemical oil extraction using n-hexane as an oil solvent. The study found that seed preparation has a significant impact on oil yields, especially in the screw press extraction method. Kernels prepared to 15% moisture content provided the highest oil yields for both extraction methods. Mechanical extraction using the screw press can produce oil from correctly prepared product at a low cost, however overall this method is ineffective with relatively low oil yields. Chemical extraction was found to be a very effective method for oil extraction for its consistence performance and high oil yield, but cost of production was relatively higher due to the high cost of solvent. However, a solvent recycle system can be implemented to reduce the production cost of Beauty Leaf biodiesel. The findings of this study are expected to serve as the basis from which industrial scale biodiesel production from Beauty Leaf can be made.

Keywords: Beauty Leaf, second generation biodiesel, bio oil extraction

1. Introduction

Demand for energy is increasing every day due to the rapid growth of population and urbanisation. Biomass is emerging as one of the promising environmentally friendly renewable energy options if the major conventional energy sources like petroleum oil, coal and gas become depleted. Biomass can be converted into liquid and gaseous fuels through thermo-chemical and biological methods. Fuels produced from these technologies are referred to as biofuels. It is generally held that biofuels offer many benefits over conventional petroleum fuels, including availability from locally available biomass sources, reduction of greenhouse gas emission, biodegradability, and contributing to sustainability [1]. However, biofuels

* Corresponding author. Md. Jahirul Islam (Jahirul M. I.) Tel.: +61(0)413809227
E-mail address: md_jahirul@yahoo.com ; mj.islam@student.qut.edu.au

contain oxygen levels of 10–45% by mass while petroleum has essentially none. This makes the chemical properties of biofuel more favorable for complete combustion. In addition, biofuels from all sources have very low sulphur content and many have a low nitrogen level which make them more eco-friendly [2]. As a consequence, biodiesel is widely used as an alternative fuel for diesel engines, whereas ethanol is used to replace gasoline [3]. In general, biodiesels are fuel obtained through the esterification of oil derived from plants or animal fat. While the biodiesel properties are comparable to regular petrodiesel, the primary difference is they are not derived from petroleum sources such as crude oil.

Currently, the sources of biodiesel under investigation include soybean oil [4], sunflower oil, corn oil, used fried oil, olive oil, rapeseed oil [5], castor oil, lesquerella oil, milkweed seed oil [6], Jatropha curcas, Pongamia glabra (karanja), Madhuca indica (mahua) [7] and palm oil [8]. These are usually produced from edible oil feedstock and are known as first generation biodiesels [9]. The most contentious issue affecting the production of first generation biodiesel is the use of agricultural land for biodiesel production. This issue is commonly referred to as the "Food verses Fuel" debate, in which the main two issues are the use of edible crops for biodiesel production, and the amount of land space devoted to growing inedible crops. Therefore an alternative must be considered which eliminates the disadvantages of first generation biodiesels. Research is currently taking place on second generation biodiesels which are targeted at addressing the "Food verses Fuel" debate [10]. However, the current production of the above mentioned feedstock does not come close to a value representative of replacing fossil fuel use. This is more prevalent when land use and potential yields are considered, which eventually affects the feasibility of biodiesel production on an industrial scale. In a recent study [11], a large number of native species have been assessed for growth on degraded land in Australia which produces biodiesel at appreciable quantities. Among them, Beauty Leaf (*Calophyllum inophyllum*) has been identified as the most suitable feedstock for future generation biodiesel feedstock. However, its potential as a source of second generation biodiesel is yet to be assessed due to a lack of knowledge of the production process. This study aims to describe the optimised oil extraction process from Beauty Leaf seeds in terms of seed preparation, moisture content and oil extraction methods.

2. Beauty Leaf (Calophyllum Inophyllum) plant

Calophyllum inophyllum, or more commonly known as Beauty Leaf, is a moderate sized tree that grows between 8–20 m tall and is most notable for its decorative leaves and fragrant flowers, as can be seen in Fig 1. The tree grows in tropical and sub-tropical climates (typical temperature range of 18–33^{o}C) close to sea level. Beauty Leaf trees grow in free draining soils near shorelines; however, it has been seen to grow in various different clay soils both within Australia (Fig.1) and various parts of southern and more central Asia such as Sri Lanka and India [12]. It is a moderately quick growing tree that can grow up to 1 m tall within a year. It has also been seen to flourish even with the presence of weeds and other species, so the plant can be grown in mixed cultures and weeding is not necessary [13]. The tree bears fruit twice a year and a healthy tree produces around 8,000 fruits which contain a kernel within a hard husk. The fruits can be harvested either directly from the tree once they are fully matured or once they have fallen off. As it has been noted that a number of animals eat the fruit, it is a safe practice to harvest the fruits from trees just before they fully mature. The kernels themselves are contained in a hard shell, as seen in Figure 1. The kernels extracted from the fruit have a dry weight of about 5 g. With around 4,000 fruits per harvest (or 8,000 per year, as fruits are produced twice a year), this results in around 40 kg of kernels per tree per year. The spacing of the trees should be 5 x 5 m, allowing 400 trees per hectare. With 400 trees per hectare, a total of 16,000 kg of kernels can be produced per year. These kernels contain about 25–60% useful oil on a unit mass basis with an average of 30%, which means each tree can yield approximately 18.4 kg of oil, thus resulting in about 4800 kg of oil per hectare per year [13].

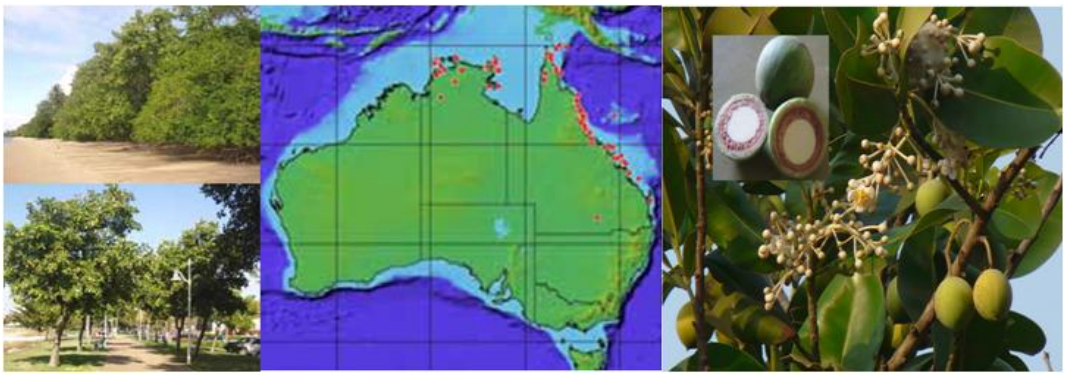

Fig. 1 - *Calophyllum Inophyllum* fruit, growing along a beach front, and in a park and its distribution in Australia

3. Seed preparation

Approximately 140 kg of seeds had been procured from Australian native plant seed suppliers. These seeds were in a ground-dried state (i.e. had been on the ground for some time prior to collection). In this state the flesh was not present with the endocarp being the outermost layer. Furthermore, the kernels had shrunk somewhat from their fresh state and so a rattle could be heard when seeds were shaken.

3.1. Kernel extraction

Preparing the seeds for oil extraction involved first removing the outer layers to expose the kernel. It was necessary to crack the seeds open in order to obtain kernels for further preparation and processing. The seed cracking process used two methods: stompers and mallets. For the stomper, a large number of seeds were placed on the ground and worked until a number had been cracked, then the kernels and the waste husk were removed. For the mallet, operators placed a handful of seeds on the table surface and cracked them individually, before removing the kernels and the waste husk (Figure 2).

For the complete 140 kg of procured product approximately 51 kg of usable kernels were obtained. This translates to approximately 36% of the total procured mass being usable kernels. Small quantities of kernels had been used for some preliminary testing, so the as-cracked figure was slightly higher than 51 kg, but certainly not 60 kg as was predicted using the small-scale testing result. From this result it was concluded that the small scale test was simply not truly representative. One possible reason for this could be the location in the seed pile that the sample was taken from. It was also found that rubber-headed mallets were preferred less than wooden or steel-headed mallets, as they tended to rebound excessively. Using mallets meant that seeds were cracked either individually or only several at a time, whereas the stomper was capable of cracking numerous seeds at a time. However, due to the variability in size of the seeds, the efficacy of the stomper was reduced as it only struck the largest seeds with each blow. Overall, kernel extraction was found to be a time-consuming and labour-intensive process. It has been estimated that each method was roughly equal in cracking rate, at approximately 2–3 kg of seeds cracked per operator per hour; however cracking process may be automatable to increase the cracking rate.

Fig. 2. Beauty Leaf seed cracking area

3.2. Kernel drying

Experiment has been conducted to investigate the optimum moisture content of the seed kernel for high oil yield. Additionally, mulched and unmulched kernels were also investigated to determine the effect of mulching on the rate of drying. The drying process was conducted using a laboratory scale Clayson electric oven with temperature controller, as shown in Figure 4. Kernels were placed in the foil trays; generally 2 kg per tray to ensure the product was spread adequately for uniform drying in an oven (Figure 3). The drying progress was checked by weighing the trays several times daily when possible, and the mulched samples were also stirred at these times to provide aeration for uniform drying. When the samples had reached their desired dryness, they were immediately removed, bagged and placed in a refrigerated store room. Both mulched and unmulched kernels were dried at 50° C and 70° C to investigate the effect of mulching on drying rate and also temperature on drying rate. One sample has been dried for as long as possible to determine the absolute moisture content of the kernels. The kernel sample were obtained with about 9.5%, 15%, 20%, 25%, and 27% moisture content which were used to investigate the effect of moisture content on bio-oil production.

Fig. 3 – Drying oven (left) and kernel trays inside (right)

For the drying rate comparison, the percentage dried was plotted against the drying time for both the mulched and unmulched samples, as shown in Figure 4. The result showed that the drying rate is higher for mulched samples. Drying of unmulched samples was roughly linear compared with mulched samples. The mulched sample also exhibited linearity although with a steeper gradient of just under 30% dryness achieved, at which point it began to plateau to a maximum of approximately 32%. For the same drying time (120 hours) the mulched sample was dried by approximately 32% while the unmulched sample was only dried by approximately 19%. The 70°C unmulched sample can be seen to dry at a higher rate compared with the 50°C unmulched sample. Again, these results are expected as drying a similarly prepared product at a higher temperature results in a faster drying rate. Interestingly, the drying characteristics are similar for the 70°C unmulched sample and the 50°C mulched sample. Therefore these results illustrated that kernel preparation could be an important factor in preparing efficient drying. Furthermore, it was noted that the maximum dryness achieved was approximately 32% which was adopted to be the absolute moisture content of the kernels. But this may vary depending on season session, location and maturity of the seeds.

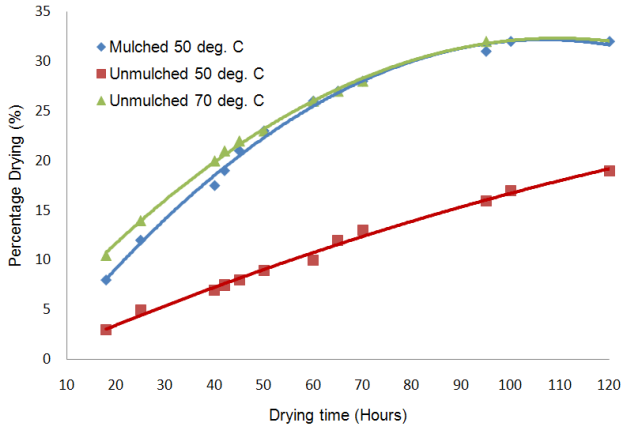

Fig. 4. Beauty Leaf seed kernel drying rate at 50 °C (mulched and unmulched) and 70 °C (ummulched)

4. **Oil extraction**

Two methods have been used for extracting oil from the prepared seed kernel. These are mechanical oil extraction using an electric powered screw press, and chemical oil extraction using n-hexane as a solvent. In both cases, experiments were conducted to find out the optimised moisture content for high oil yield.

4.1. Mechanical oil extraction

The mechanical oil extraction and experiment were conducted using a Mini 40 screw press at CPWS, Central Queensland University (CQU). As the screw press (Figure 5a) used in this study was not designed for Beauty Leaf seeds, it was realised that using this press for the oil extraction not only would this be challenging, but would require a degree of experimentation to adjust pressure and speed. Some modification also has been done to control proper operation. For example, glad wrap was used around the machine to capture any spilt material for the specific purpose of keeping mass control as precise as possible in order to give the most valid oil yield results.

(a) (b)

Figure 5: (a) Mechanical oil extraction through a screw press (b) Chemical oil extraction

Beauty Leaf kernel was found to be very difficult to process using the screw press. Two operators were required to constantly attend to the machine and the rate of oil production was very low, typically taking over an hour to process just one sample. However, there was a noticeable increase in workability; as the samples became drier; oil was extracted much earlier so the extraction process was less laborious. The most consistently high oil yields were produced with 15% absolute moisture content, as shown in Figure 7. However, further improvement of Beauty Leaf oil extraction using the screw press is possible by optimising key design parameters of the machine including pressure, compression ratio, speed, and hot pressing.

4.1. *Chemical oil extraction*

For chemical oil extraction, dried seed kernels samples were ground using the blender and coffee grinder to obtain a fine consistency to maximise particle surface area. The ground kernels were put into conical flasks in which hexane were added at a ratio of 2:1 (mL hexane: grams kernel). The mixture was given an initial stir to ensure that all kernels were wetted with hexane. Conical flask openings were covered with aluminium foil and placed on the orbital mixer under the fume hood for safety reasons, and the samples were left to run for at least eight hours. Then the hexane/oil mixtures were collected, filtered and decanted into aluminium foil containers for solvent evaporation, and placed under the fume hood (Fig. 5b) for eight to 10 hours. Hexane was again added to the conical flask of kernels, but at a ratio of 1:1 for the second extraction, and a similar procedure was followed for recovery of the oil. When it was determined that the hexane had been fully evaporated, the oil was transferred into containers for analysis.

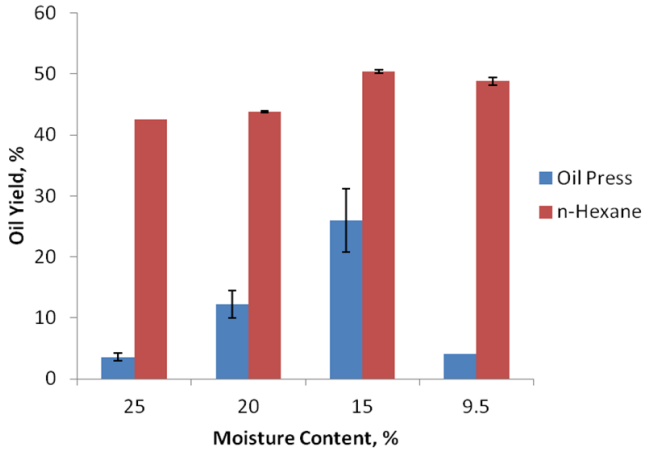

Figure 7: Oil yield against absolute moisture content for chemically and mechanically processed samples

In terms of oil yield from the two extraction methods, hexane oil extraction was vastly more successful. For the test sample extractions (referring to Fig. 7), the samples with 15% absolute moisture content produced the highest oil yields, averaging approximately 51% (with respect to input dry mass). The difference was only slight between samples with an absolute moisture content of between 10% and 15%. However, the biggest obstacle for the hexane extraction method is the cost of the solvent. Therefore, is it strongly recommended to use the n-hexane recovery system to reduce the production cost of bio-oil production through the chemical method.

Table 1- Advantages and disadvantages of the two extraction methods

Mechanical Extraction		**Chemical Extraction**	
Advantages	***Disadvantages***	***Advantages***	***Disadvantages***
• Virgin oil is more sought after • No potential for solvent contamination • Relatively inexpensive after initial capital costs • Minor consumables cost	• Generally ineffective for processing Beauty Leaf • Time and labour intensive • Relatively low oil yields • Operators require experience to achieve best results • High dependence on kernel moisture content	• Repeatable and reproducible results and process • High oil yields • Relatively simple and quick • Hexane can be recovered and reused, reducing cost significantly	• Less sought after than virgin oil • Potential for solvent contamination • Safety issues and environmental concerns regarding the use of hexane • Very costly if the hexane cannot be recovered

5. **Comparison of oil extraction methods**

The results from the mechanical and chemical extraction methods clearly indicate that the hexane method is superior in terms of producing higher oil yields. It was also observed that the chemical method is more repeatable, relative ease of preparation and no requirement for extensive training. However, seed preparation has a significant impact on oil yields especially for the screw press extraction method. Kernels prepared to 15% moisture content provided the highest oil yields for both extraction methods. Mechanical extraction using the screw press can produce oil from appropriately prepared product, but overall this method is ineffective, with relatively low yields for a great deal of effort. Chemical extraction using hexane as a solvent was found to be very effective, but due to a limited supply of hexane and the lack of a hexane recovery system, it was not possible to take full advantage of the effectiveness of the method. Therefore, it is recommended to use chemical oil extraction with the hexane recovery system to reduce production cost of Beauty Leaf biodiesel. Moreover, as evidenced by the bulk extraction results, the hexane method proved to be a vastly more time and labour efficient process than mechanical extraction in the given circumstances. The advantages and disadvantages oil extraction methods observed in this study are summarised in Table 1.

6. **Conclusion**

Seed processing, drying and oil extraction methods a significant impact on oil yields and the success of Beauty Leaf as future generation biodiesel feedscock. Drying the seed kernel to optimum moisture content was found to be crucial to the success of both mechanical extraction and hexane extraction. Kernels prepared with 15% moisture content provided the highest oil yields for both extraction methods. Mechanical extraction using the screw press is ineffective, with relatively low yields for a great deal of effort. Chemical extraction using hexane as a solvent was found to be very effective, however due to a limited supply of hexane and the lack of a hexane recovery system, it was not possible to take full advantage of the effectiveness of the method. Therefore it is recommended to use chemical oil extraction with hexane recovery system to reduce the production cost of Beauty Leaf biodiesel. Though less crucial than hexane recovery, it is noted that kernel preparation was the most time consuming element of the hexane extraction process experienced during the project. Therefore, a potential area for improvement or a possible future project would be to investigate streamlining/automating and up-scaling the kernel preparation process.

References

[1] Rajindars L., 2006. Conditions for the sustainability of biomass based fuel use. Energy Policy 34(7), p. 863-876.
[2] Hoekman, S. K., Broch, A., Robbins, C., Ceniceros, E., & Natarajan, M. 2012. Review of biodiesel composition, properties, and specifications. Renewable and Sustainable Energy Reviews, 16(1), p. 143-169.
[3] Demirbas, A., 2007. Progress and recent trends in biofuels. Prog. Energ. Combust. 33 (1): p.1-18
[4] Goodrum J. W. and Geller D. P., 2005. Influence of fatty acid methyl esters from hydroxylated vegetable oils on diesel fuel lubricity Bioresource Technology. 96, p 851–855.
[5] Terry, B. 2005. Impact of Biodiesel on Fuel System Component Durability. The Associated Octel Company Limited. Technical Report, FTC 2005.01
[6] Holser, R. A. & Harry-o'kuru, R. 2006. Transesterified milkweed (Asclepias) seed oil as a biodiesel fuel,. Fuel,; 85**,** p 2106-2110.
[7] Kaul, S., Saxena, R. C., Kumar, A., Negi, M. S., Bhatnagar, A. K., Goyal, H. B. & Gupta, A. K., 2007. Corrosion behavior of biodiesel from seed oils of Indian origin on diesel engine parts. Fuel processing technology, 88**,** p 303-307.
[8] Raadnui S., Meenak A., 2003, Effect of refined palm oil (RPO) fuel on wear of diesel engine components, Wear, 254, p 1281-1288.
[9] Rashid, U., Anwar, F., 2008. Production of biodiesel through optimized alkaline-catalyzed transesterification of rapeseed oil. Fuel, 87(3), p 265-273
[10] Bradsher, K., 2008. The other oil shock: Vegetable oil prices soar. The New York Times, January 19, 1. World Business.
[11] Ashwath, N., 2010. Evaluating Biodiesel Potential of Australian Native and Naturalized Plant Species. RIRDC Publication No. 10/216. ISBN: 978-1-74254-181-5.
[12] CSIRO, 2010. (Australian Government, CSIRO, and Reef & Rainforest Research Centre, "Calophyllum inophyllum," Australian Tropical Rainforest Plants, 6 no. 1.
[13] Okano D. Friday J. B., 2006. Calophyllum inophyllum (kamani),"Species Profiles for Pacific Island Agroforestr,; 2: no 1

Available online at www.sciencedirect.com

SciVerse ScienceDirect

Procedia Engineering 00 (2012) 000–000

Procedia Engineering

www.elsevier.com/locate/procedia

5th BSME International Conference on Thermal Engineering

Biodiesel from Neem Oil as an Alternative Fuel for Diesel Engine

Md. Hasan Ali[a]*, Mohammad Mashud[b], Md. Rowsonozzaman Rubel[b], Rakibul Hossain Ahmad[b]

[a]*Department of Energy Technology, Khulna University of Engineering & Technology, Khulna-9203, Bangladesh*
[b]*Department of Mechanical Engineering, Khulna University of Engineering & Technology, Khulna-9203, Bangladesh*

Abstract

In the current energy scene of fossil fuel, renewable energy sources such as biodiesel, bioethanol, biomethane, and biomass from wastes or hydrogen have become the subjects of great interest. These fuels contribute to the reduction of dependence on fossil fuels. In addition, energy sources such as these could partially replace the use of those fuels which are responsible for environmental pollution and may be scarce in the future. For these reasons they are known as "alternative fuels". Vegetable oil cannot be directly used in the diesel engine for its high viscosity, high density, high flash point and lower calorific value. So it needs to be converted into biodiesel to make it consistent with fuel properties of diesel. Biodiesel production is a valuable process which needs a continued study and optimization process. The present study was intended to consider aspects related to the production of biodiesel from Neem oil and investigating its fuel properties. The seeds of Neem contain 30-40 % oil. This report deals with biodiesel obtained from Neem oil which are mono alkyl esters produced using ***'Transesterification'*** process. The optimum conditions to achieve maximum yield of biodiesel were investigated at different temperatures and with different molar ratio of Neem oil and methanol. The most expected result including layer of glycerin and soap has been investigated at 3:1 molar ratio of methanol and Neem oil at 55 to 61°C temperature ranges. It was apparent that the fuel properties of biodiesel including density, kinematic viscosity and calorific value lie within the standards biodiesel properties especially (ASTM 6751-02) recommended standard of kinematic viscosity lies between 1.90 to 6.0 centistokes. Biodiesel can make a major contribution in the future if it meets the few percent of petroleum and it can provide improved fuel properties lower emission of unburned hydrocarbons, carbon monoxide but higher level of oxides of nitrogen.

Keywords: Biodiesel; Neem Oil; Ethyl Ester; Free Fatty Acid, Transesterification

1. Introduction

In the modern world, the demand for non-renewable energy sources is increasing day by day due to modernization and mechanization. Demand for electricity and enormous increase in the number of automobiles has resulted in greater demand for petroleum products. The increasing demand for the petroleum based fuels has led to oil crises in the recent times. Therefore attention has been focused on developing the renewable or alternate fuels to replace the petroleum based fuels for transport vehicles.

Fossil fuels are still being created today by underground heat and pressure; they are being consumed more rapidly than they are being created. Insufficient quantities or unreasonable price of petroleum fuels deeply concerns us whereas the renewable energy is a promising alternative solution because it is clean and environmentally safe [1].Due to petroleum fuel, Pollution and accelerating energy consumption have already affected equilibrium of the earth's landmasses and biodiversity.

* Corresponding author. Tel.: +88-01818555598
E-mail address: mhakuet@yahoo.com

Since petroleum diesel and gasoline consist of blends of hundreds of different chemicals of varying hydrocarbon chains, many of these are hazardous and toxic. Carbon monoxide (produced when combustion is inefficient or incomplete), nitrogen oxides (produced when combustion occurs at very high temperatures), sulfur oxides (produced when elemental sulfur is present in the fuel), and particulates that are generally produced during combustion are other specific emissions of concern. So it is time to search for its alternative fuels [2].There are several alternative sources of fuel like vegetable oils, biogas, biomass, primary alcohols which are all renewable in nature. Among these fuels, vegetable oils appear to have an exceptional importance as they are renewable and widely available, biodegradable, non-toxic and environment friendly. The alternative fuel that much closer to diesel engine is 'biodiesel'.

Biodiesel refers to a family of products made from vegetable oil or animal fats and alcohol, such as methanol or ethanol, called mono alkyl esters of fatty acids. Study shows that, on the mass basis, biodiesel has an energy content of about 12% less than petroleum based diesel fuel. It reduces unburned hydrocarbons (HC), carbon monoxide (CO), and increase oxides of nitrogen (NO_x) than diesel-fueled engine. It is a domestic, renewable fuel for diesel engine derived from natural oil like Neem oil. Biodiesel is environment friendly liquid fluid similar to conventional diesel fuel in engine tests, the power and fuel consumption [3, 4].

Neem is a tree in the family 'maliaceae' which grows various parts in Bangladesh. It's scientific name '*Azadirachta indica'*. The evergreen tree is large, reaching 12 to 18 meters in height with a girth of up to 1.8 to 2.4 meters. The seeds have 40% oil which has high potential for the production of biodiesel. It has a higher molecular weight, viscosity, density, and flash point than diesel fuel. Neem oil is generally light to dark brown, bitter and has a strong odor that is said to combine the odors of peanut and garlic [5,6].

Neem comprises mainly of triglycerides and large amounts of triterpenoid compounds. It contains four significant saturated fatty acids, of which two are palmitic acid and two are stearic acid. It also contains polyunsaturated fatty acids such as oleic acid and linoleic acids [7].

2. Biodiesel Production Methods

The present study is based on biodiesel production which consists of reaction where an ester reacts with alcohol to form another ester and another alcohol. Ester here is the vegetable oil (Neem oil) which consist triglyceride. There are four ways to use neat vegetable oils in diesel engine [10-13]:

i. Direct use or blending in diesel fuel
ii. Micro emulsions in diesel fuel
iii. Thermal cracking of vegetable oils
iv. Transesterification.

Out of the four methods, *transesterification* is the most popular and best way to use neat vegetable oils [14]. It was conducted as early as 1853 by scientists E. Duffy and J. Patrick, many years before the first diesel engine became functional [14]. For the purpose of soap production, in the 1940s this process was developed to improve the separation of glycerin [16]. Acid catalyst is used for the esterification and alkali catalyst was (KOH or NaOH) used for the transesterification reaction. The formation of methyl esters by transesterification of vegetable oil requires raw oil, 15% of methanol & 5% of sodium hydroxide on mass basis. On mol basis, one mol glyceride reacts with three mol methanols in presence of a catalyst (KOH or NaOH) to produce methyl esters. For the equilibrium condition of the reaction 55-65°C temperature is needed. In most cases the temperature is kept below the normal boiling point of the methanol (65°C), so that the reactor does not need to be pressurized [3,17].

The Total Process Followed Two Stages:

Firstly, to reach the equilibrium conditions at temperature 55-65°C. Secondly, for glycerin separation the product mixture was stimulated continuously and then allowed to settle under gravity in a separating funnel [3, 16]. Two distinct

layers form after gravity settling for 24h. The upper layer was of ester and lower layer was of glycerol. The lower layer was separated out. The separated ester contains 3% to 6% methanol and usually some soap. If the soap level is low enough (300 to 500 ppm), the methanol can be removed by vaporization and this methanol will usually be dry enough to directly recycle back to the reaction. After the removal of methanol, the biodiesel needs to be washed to remove residual free glycerin, methanol, soap, and catalyst. It is done frequently before creating emulsion of contaminants themselves. Biodiesel was mixed with some warm water (around 10 % volume of ester) to remove the catalyst present in ester and allowed to settle under gravity for another 24h. The catalyst gets dissolved in water, which is separated and removed the moisture. The washing process is usually done multiple times until the wash water no longer picks up soap [4, 18].

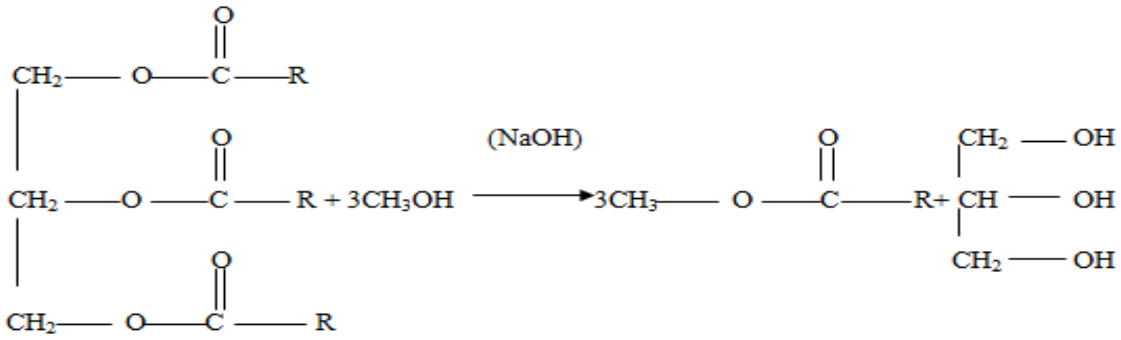

Where, R is long chain hydrocarbons.

Although the gray water from later washes can be used as the supply water for the earlier wash steps, the total amount of water will typically be one or two times the volume flow rate of the biodiesel. I used 10% of water of total volume of biodiesel and heated above 100°C. The residual methanol and water both were vaporized. Acids can be used to reduce the amount of water. Weaker organic acid, such as citric acid, will neutralize the catalyst and produce a soluble salt.

Stronger inorganic acid such as hydrochloric, sulfuric, or phosphoric, can be used to split the soap and this reduces the water requirement to 5% to 10 % of the biodiesel because the salts are easier to remove than the soap. The residual water droplets of biodiesel after settling out can be removed by flash evaporator. Although I applied water washing technique for separation of residual methyl esters but instead of using water washing, solid absorbents such as magnesium silicate can be used for this purpose. The fine powder of absorbents absorbs the contaminants such as soap, catalyst, and free glycerol. [4].

The overall processing of biodiesel from Neem oil consists of the collection of oil from Neem seeds first. Combined reaction of alcohol, catalyst &oil takes place. Catalyst works here as the unchangeable compound which runs the reaction speedy well. The schematic diagram of the production of biodiesel from oil is given bellow:

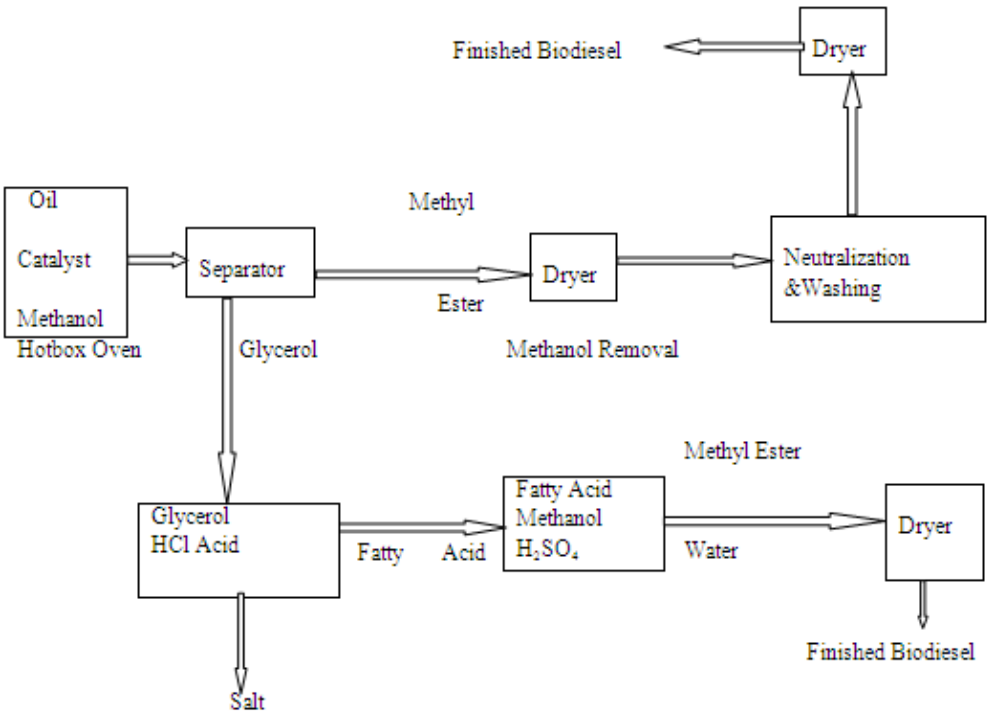

Fig.1. Schematic of Biodiesel Processing

When the separation of esters and glycerol occurs, glycerol contains soaps, catalyst, methanol & other impurities. So for the improvement of this situation, purity of the glycerol is needed. To neutralize the catalyst and split the soap strong hydrochloric acid (HCl) was added to the glycerin [4].

$$\text{Soap} + \text{Hydrochloric Acid} \longrightarrow \text{Fatty Acid} + \text{Salt}$$

In the glycerin, the free fatty acids are not soluble; so it can be easily separated using a centrifuge. Methanol can be removed by vaporization. Remainder impurities are salt. There is a special concern that high free fatty acid (FFA) during biodiesel production may cause obstruction to the separation of methyl esters and glycerin.

$$\text{Fatty Acid} + \text{NaOH} \longrightarrow \text{Soap} + \text{Water}$$

$$\text{Fatty Acid} + \text{Methanol} \xrightarrow{H_2SO_4} \text{Methyl Ester} + \text{Water}$$

The acid based catalization slows the transesterification reaction. The two-step approach of acid-catalyzed esterification followed by base-catalyzed transesterification gave a complete reaction at moderate temperature (50 to 61°C). The biodiesel we need was processed finally by drying the found methyl ester [3, 4, 16, 17].

3. The experimental investigation

This was performed in the metrology lab, Department of Mechanical Engineering, KUET, Bangladesh. Oil samples with beaker were kept on hotbox oven chamber. Amongst all the samples we take one as the most satisfactory result. The sample of 100 ml of Neem oil with 300 ml of methanol (CH_3OH) in presence of N_aOH as catalyst was taken as final production of biodiesel. The amount of biodiesel was 0.95 ml. The viscosity was measured with the help of Say bolt Viscometer. The density and calorific value were measured with the help of Electronic Precision Balance and Bomb Calorimeter respectively in the Heat Engine Laboratory. In the following figure it shows the stage of biodiesel with glycerin and soap layer which was found at equilibrium condition.

Fig 2. Biodiesel processing in Hotbox Oven Chamber

Fig. 3. Shows the different layers after reaction

Table 1. The observed properties

Properties	Neem oil	Neem oil*	Biodiesel	Diesel*
Density (gm/cc)	0.878	0.778	0.61	0.84
Kinematic viscosity (centistokes) at 35°C of oil	24.14	21.38	5.96	4.0
Calorific value [MJ/kg]	26.65	_	38.15	45

* Properties are taken as standard value

Reduction in viscosity (24.14-5.96) = 18.18 centistokes. As the viscosity is the vital factor for oil being consistent to be used as diesel so the reduced viscosity made the Neem oil to biodiesel as it lays the ASTM D6751-02 recommended standard of 1.90 to 6.0. Other properties i.e. density, calorific value were also taken but not mentioned in the tables.

Table 2: Cost of biodiesel production from Neem oil:

SI. No.	Component	Cost (Tk.)
1	Neem Oil – 100 ml	8.25
2	Transesterification Cost- 300 ml of Methanol	216
3	Catalyst NaOH 0.8 gm	1.10
4	Recovery (Glycerin 100 ml+ Soap 190 ml)	50
5	Total Cost	175.35

Biodiesel production from 1 liter Neem Oil=0.95 Liter
So Cost of Biodiesel per liter= 1845.78 Tk.

The cost of the biodiesel production can be minimized as possible to recover the used methanol. Recycling of methanol again and again in mass production and commercial use the cost must be come to the lowest amount. Also the by-product such as glycerin and soap play an important role to minimize the cost.

4. Discussion

The use of biodiesel as an alternative fuel has turned the technological aspect of energy evaluation to a growing change. The conversion of vegetable oil such as Neem oil to biodiesel has performed and a remarkable change of the fuel properties were observed. From the observed properties of biodiesel it is shown that properties were very close to diesel properties. During the production of biodiesel from Neem oil, the challenge is to reduce the cost of production low enough that it can compete with diesel, which will come as biodiesel producers improve and automate production operations. The layer formation here is the concerning matter because of the proper transesterification may hamper due to absence of proper amount of methanol and catalyst. The reaction consumes about 6 to 7 hours to come into equilibrium condition. The 3:1

molar ratio of methanol and oil at 55°C to 61°C (below 65°C) in presence of 1 atm pressure has been found as the expected condition for equilibrium. The hard formation of glycerin and soap layer contributes to the most appropriate biodiesel production. The separated by product can give economical support which is one of the advantageous aspect of biodiesel production. Being introduced with the property investigations it can be explained that Neem oil has low properties of using as fuel but the formation of biodiesel from it leads it to use as an alternative fuel for diesel engine. The observed properties intended me to use it as the future generation fuel in assistance with the petroleum based fuel specially diesel fuel. Kinematic viscosity is the main thing for biodiesel specification. As the observed kinematic viscosity lay between 1.9 to 6.0 according to the ASTM D6751 specification so my produced biodiesel was suitable for using in diesel engine.

5. Conclusion

Biodiesel is a domestic fuel alternative and can contribute to a more stable supply of energy. The biodiesel fuel production process has evolved considerably to minimize the original problems with viscosity. Today, biodiesel is an increasingly attractive, non-toxic, biodegradable fossil fuel alternative that can be produced from a variety of renewable sources. Neem oil has potential as an alternative energy source. But it is not possible for oil alone to solve dependency on foreign oil within any particular time frame. Significant commitment of resources would require increasing production of Neem oil. These needs are being met with recent advances in instrumentation technology. The emphasis should be made to invest in agriculture sector for exploitation of existing potential by establishing model seed procurement centers, installing preprocessing and processing facilities, oil extraction unit, transesterification units etc. The organized plantation and systematic collection of Neem oil, being potential bio-diesel substitutes will reduce the import burden of crude petroleum.

Rferences

[1] Ayhan Demirbas, 'Biodiesel: A Realistic Fuel Alternative for Diesel Engines', Sila Science and Energy, Trabzon, Turkey, (May, 2007), pp. 2-7.

[2] K.V.Radha, G.Manikandan, ' Novel Production Of Biofuels From Neem Oil', (2011) Department of chemical Engineering, Anna University, Chennai, India.

[3] Jon H. Van Gerpen, Charles L. Peterson, Carrol E. Goering, Biodiesel: An Alternative Fuel for Compression Ignition Engines, for presentation at the 2007 Agricultural Equipment Technology Conference Louisville, Kentucky, USA 11-14 February 2007.

[4] Asadullah Al Galib and Md. Roknuzzaman, March 2009 'Biodiesel from Jatrofa oil as an alternative fuel for Diesel Engine', KUET, Khulna, Bangladesh.

[5] M. Shahin-uz-zaman1, M. Ashrafuzzaman, M. Shahidul Haque and Lutfun Nahar Luna, 2007 'In vitro clonal propagation of the neem tree (Azadirachta indica A. Juss.)', BAU, Bangladesh.

[6] M.A. Fazal, A.S.M.A. Haseeb and H.H. Masjuki. (2011) 'Biodiesel feasibility study: An evaluation of material compatibility; performance; emission and engine durability', Renew. sustain.Engy Reviews, Vol.15,2, 1314-1324

[7] Muthu1, V. SathyaSelvabala1, T. K. Varathachary2, D. Kirupha Selvaraj1,J. Nandagopal2 and S. Subramanian1 'synthesis of biodiesel from neem oilusing sulfated zirconia via tranesterification'.

[8] E. Crabbe, C. Nolasco-Hipolito, G. Kobayashi, K. Sonomoto and A. Ishizaki. 2001. Biodiesel production from crude palm oil and evaluation of butanol extraction and fuel properties. Process Biochemistry. 37: 65-71.

[9] G. Knothe and K.R. Steidley. 2005. Lubricity of components of biodiesel and petrodiesel: The origin of biodiesel lubricity. Energy and Fuels. 19: 1192-1200.

[10] Fangrui Ma, and Milford A Hanna, Biodiesel Production: a Review, *Bioresource Technology, 70 (*1999), pp.1-15.

[11] Agarwal A K. Biofuels (alcohols and biodiesel) applications as fuels for internal combustion engines, *Progress in Energy and Combustion Science*, 33 (2007), pp.233–271.

[12] Graboski, M S, and Mc Cormick, R L., Combustion of fat and vegetable oil derived fuels in diesel engines, *Prog. Energy Combust. Sci*, 24 (1998), pp.125-164.

[13] Anjana Srivastava, Ram Prasad., Triglycerides – based diesel fuels. *Renewable and Sustainable Reviews*, 4 (2000), pp.111-133.

[14] F. Ma and M.A. Hanna. 1999. Biodiesel production: a review. Bioresource Technology. 70: 1-15.

[15] http://en.wikipedia.org/wiki/Bio_Diesel

[16] Bradshaw, G. B., and W.C. Meuly. 1942. Process of making pure soaps. U.S. Patent 2,271,619.

[17] Van Gerpen, J. 2005. Biodiesel processing and production. Fuel processing Technology 86: 1097-1107.

[18] T. Wimmer, "Process for the Production of Fatty Acid Esters of Lower Alcohols," US Patent No. 5,399,731 (1995).

[19] W.D. Stidham, D.W. Seaman, and M.F. Danzer, "Method for Preparing a Lower Alkyl Ester Product from Vegetable Oil," US Patent No. 6,127,560 (2000).

[20] Foglia, T.A., Jones, K.C., Haas, M.J. and Scott, K.M. (2000) 'Technologies supporting the adoption of biodiesel as an alternative fuel. The cotton gin and oil mill presses.

Available online at www.sciencedirect.com

SciVerse ScienceDirect

Procedia Engineering 00 (2012) 000–000

Procedia Engineering

www.elsevier.com/locate/procedia

5th BSME International Conference on Thermal Engineering

Nanoparticle Enhanced Ionic Liquids (NEILs) as Working Fluid for the Next Generation Solar Collector

Titan C. Paul[a], AKM M. Morshed[a], Jamil A. Khan[a*]

[a]*Department of Mechanical Engineering, University of South Carolina, Columbia, SC, USA*

Abstract

Next generation solar thermal collector requires working fluid with high heat storage capacity as well as high temperature thermal stability to reduce its operating cost. Ionic liquids (ILs) are considered as a potential working fluid for next generation solar collector due to suitable thermophysical properties. However, Nanoparticle Enhanced Ionic Liquids (NEILs), a class of nanofluids, can further enhance the thermophysical properties of ILs. In this study, an experimental assessment on NEILs was performed by measuring thermophysical property and evaluating forced convection performance. Experimental results show clear advantages of the NEILs over the base ILs both in heat storage capacity and heat transfer performance. Up to 6% enhancement in thermal conductivity, 23% enhancement in heat capacity, and 20% enhancement in convective heat transfer performance has been observed for the 1% (Weight%) aluminium oxide (Al_2O_3) enhanced ILs compared to the base ILs. Our current study lays the foundation for future studies to explore further investigation to evaluate NEILs as a potential working fluid for the next generation solar collectors.

Keywords: Nanoparticle Enhanced Ionic Liquids (NEILs); Thermal Conductivity; Heat Capacity; Heat Transfer Coefficient.

Nomenclature

K	thermal conductivity (W/m.K)
C_p	heat capacity
Re	Reynolds number

Greek symbols

Φ	volume fraction

Subscripts

BL	base liquid
NEIL	Nanoparticle Enhanced Ionic Liquid
n	Nanoparticle

1. INTRODUCTION

Heat transfer fluid (HTF) is defined as the gas or liquid which can transmit heat energy from one system to other. One of the important uses of these HTF is in Concentrating Solar Power (CSP) system, where mirror or lances is used to concentrate sunlight from a large area and store in the HTF. Later on energy of this HTF is used to produce steam for power

* Corresponding author. Tel.: +1-803-777-1578 ; fax: +1-803.777.0106
E-mail address: khan@cec.sc.edu

generation [1]. The limitations of currently used HTF for CSP system (i.e. lower storage capacity and lower thermal stability) result not only lower cycle efficiency but also higher operating cost. Therefore, it is all the more important to enhance the working efficiency of HTF to achieve a cost effective efficient CSP system. Nanoparticle Enhanced Ionic Liquids (NEILs) [2-4] based HTF is considered as a potential candidate for CSP system. NEILs, a class of nanofluids, is synthesized by dispersing small amount of nanoparticles in base ionic liquids (ILs). ILs are the group of salts, which consist of organic cations (imidazolium, pyrazolium, triazolium, thiazolium, oxazdium, pyridinium, pyridazinium, pyrimidinium, pyrazinium) and organic or inorganic (halogen, fluorinated) anions and are liquid at room temperature [5]. Versatility in synthesis and excellent thermophysical properties such as wide liquid temperature range, high heat capacity, high density, negligible vapor pressure, and high thermal stability have eventually established ILs as potential replacement of current HTF for solar collector [6-11]. However, researchers are now extensively investing how to maximize the performance of ILs for solar thermal system [2-4, 12-17].

IoNanofluid, a combination of several imidazolium and pyrrolidinium based ILs and multi wall carbon nanotubes, have been reported to have higher thermal conductivity and heat capacity compared to the base ILs [12, 13]. Improved thermophysical properties were also reported using other NEILs consisted of 1-Butyl-2,3-dimethylimidazolium bis{(trifluoromethyl)sulfonyl}imide ($[C_4mmim][NTf_2]$) and aluminium oxide (Al_2O_3) nanoparticles [2], hydrophobic and hydrophilic imidazolium-based ILs and silicon dioxide (SiO_2) nanoparticles [14], gold nanoparticles based ILs [15-17], nanofluids synthesized by lithium carbonate and potassium carbonate (62:38 ratio) with SiO_2 nanoparticles [18], and alkali chloride salt eutectic with SiO_2 nanoparticles [19]. T. C. Paul et al. [3] have recently reported the ~3% enhancement of thermal conductivity of NEIL made with 1-butyl-3-methylimidazolium bis{(trifluoromethyl) sulfonyl}imide ($[C_4mim][NTf_2]$) and 0.5% Al_2O_3 nanoparticles.

Results from all the previous studies were encouraged the author to conduct the experimental assessment of the NEILs as a HTF for solar collector application. All the previous study was mainly the thermophysical property measurement of NEILs. There is no study on its heat transfer performance, which motivates to conduct the study. The experimental assessment includes thermal conductivity and heat capacity study of NEILs made with 1-butyl-3-methylimidazolium bis{(trifluoromethyl)sulfonyl}imide ($[C_4mim][NTf_2]$) and N-butyl-N-methylpyrrolidiniumbis{trifluoromethyl)sulfonyl} imide ($[C_4mpyrr][NTf_2]$) ILs and 1% Al_2O_3 nanoparticles. Heat transfer behavior of NEIL also presents.

2. Material and synthesis of the NEIL

Al_2O_3 nanoparticles (γ-phase) having particles size < 50nm (TEM) and surface area >40 m^2/g (BET) were purchased from Sigma-Aldrich, USA. 99% pure $[C_4mim][NTf_2]$) and ($[C_4mpyrr][NTf_2]$) ILs having molecular weight of 419.37 g/mol and 422.41 g/mol respectively were purchased from IoLiTec Company (Germany) Molecular formula of $[C_4mim][NTf_2]$ and $[C_4mpyrr][NTf_2]$ are $C_{11}H_{20}F_6N_2O_4S_2$ and $C_{10}H_{15}F_6N_3O_4S_2$ respectively.

NEILs were prepared by mixing 1% (by wt.) Al_2O_3 with $[C_4mim][NTf_2]$ and $[C_4mpyrr][NTf_2]$ as base ILs. Al_2O_3 nanoparticles were dispersed into the ILs using a vortex mixture and agitated for approximately 90 min to break any possible agglomerated nanoparticles.

3. RESULTS AND DISCUSSION

3.1. Enhanced thermal conductivity

Thermal conductivity of the base ILs and NEILs were measured using KD2 Pro thermal property analyzer (Decagon Device, USA). The measurements principle is based on the transient hot wire method. The meter has a probe of 60 mm length and 1.3 mm diameter with a heating element and a thermoresistor, which is inserted vertically into the test sample. The probe is connected to a microcontroller for controlling and conducting the measurements. Before taking any reading, the meter was calibrated with distilled water and standard glycerin. A thermal bath (Thermo NESLAB) was used to maintain constant temperature of the measuring sample. Temperature accuracy of the bath was within ±0.01 K.

Normalized thermal conductivity of 1% $[C_4mim][NTf_2]$ and $[C_4mpyrr][NTf_2]$ based NEILs with respect to corresponding thermal conductivity of base ILs as a function of temperature indicate that the thermal conductivity is enhanced by ~6% (for $[C_4mim][NTf_2]$) and ~5% (for $[C_4mpyrr][NTf_2]$) over the measured temperature range (Figure 1). Moreover, variation in thermal conductivity within the temperature range is insignificant. The measured thermal conductivity of both NEILs were compared with the predicted value using Maxwell's equation which was developed to determine the effective thermal conductivity of liquid–solid suspensions for spherical particles [20]:

$$\frac{k_{NEIL}}{k_{BL}} = \frac{k_s + 2k_{BL} - 2\phi(k_{BL} - k_n)}{k_s + 2k_{BL} + \phi(k_{BL} - k_n)} \quad (1)$$

where k_{NEIL}, k_{BL}, $k_n = 36\ \frac{w}{mK}$ are the thermal conductivity of NEILs, base ILs, and Al_2O_3 nanoparticles respectively; Φ is the nanoparticles volume fraction. Prediction of Maxwell's model shows lower thermal conductivity enhancement compare to the experimentally measured values (Figure 1) because Maxwell' model only consider the volume fraction and the thermal conductivity of the base liquid and nanoparticles. Particle size and interfacial liquid layer may also affect the effective thermal conductivity. Using carbon nanotubes and gold nanoparticles with different base ILs, similar trends were also reported earlier [12-13, 15-16]. Hence, more extensive investigations are required to explore the exact mechanism behind this discrimination.

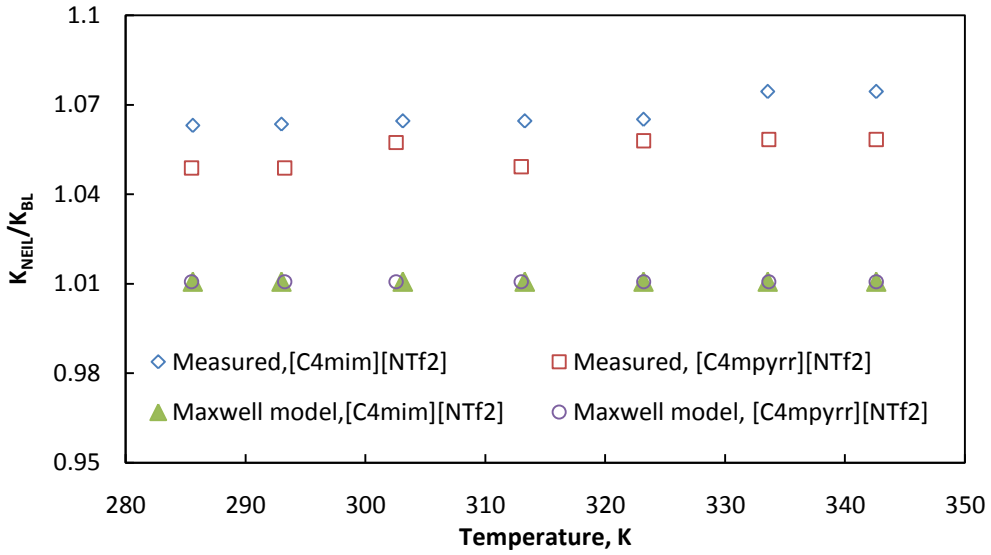

Figure 1: Normalized effective thermal conductivity of NEILs as a function of temperature

3.2. Enhanced heat capacity

Heat capacity of ILs and NEILs were measured using Differential Scanning Calorimetry (DSC Q2000 from TA instruments Inc.). The sample having average weight of 12.89 mg was placed in a standard aluminum hermetic pan covered with lid. Nitrogen was used as cooling system at flow rate of 40 mL/min and DSC was operated at a heating rate of 10°C/min. Three independent runs were performed using reported experimental procedure [18-19].

Table 1: Comparison of heat capacity of base ILs (measured) and NEILs (measured and predicted)

Temperature, K	Heat capacity (J/g.K)					
	Measured		$[C_4mim][NTf_2]$+1%Al_2O_3		$[C_4mpyrr][NTf_2]$+1%Al_2O_3	
	$[C_4mim][NTf_2]$	$[C_4mpyrr][NTf_2]$	Measured	Predicted	Measured	Predicted
298.15	1.746	1.536	2.147	1.742	1.899	1.533
323.15	1.74	1.644	2.312	1.736	2.072	1.641
348.15	1.775	1.727	2.396	1.771	2.184	1.724
373.15	1.809	1.801	2.454	1.805	2.262	1.797
398.15	1.846	1.862	2.515	1.842	2.322	1.858
423.15	1.898	1.921	2.583	1.894	2.382	1.917
448.15	1.952	1.983	2.648	1.947	2.441	1.979
473.15	1.99	2.045	2.701	1.985	2.501	2.040
498.15	2.036	2.097	2.746	2.031	2.557	2.092
523.15	2.091	2.144	2.776	2.086	2.604	2.139
548.15	2.163	2.188	2.799	2.158	2.643	2.183

Measured heat capacity of NEILs was compared with the existing theoretical model of the effective specific heat for a mixture [21]:

$$c_{p,NEIL} = \phi c_{p,n} + (1-\phi)c_{p,BL} \quad (2)$$

where, $c_{p,NEIL}$, $c_{p,n} = 0.791\ {}^{J}/_{g.K}$, and $c_{p,BL}$ are the heat capacity of NEIL, nanoparticles, and base IL respectively, ϕ is the nanoparticles volume fraction. Measured heat capacity of ILs and NEILs at 25K interval from 298K to 548K show that inclusion of NEILs has enhanced the heat capacity is by ~23%, whereas the model always predicts lower heat capacity (Table1). The significant enhancement of heat capacity of NEILs cannot be predicted by the model and more sophisticated investigations will be required to explain these enhancements. Meanwhile, similar enhancement (~26%) of heat capacity with a small amount of nanoparticles was observed earlier where synthesized silica nanofluids from lithium carbonate and potassium carbonate (62:38 ratio), and alkali chloride salt eutectic with SiO_2 nanoparticles (1% by wt.) were used [18-19]. This increment in heat capacity of NEILs is important for their potential applications as a HTF for CSP system.

3.3. Enhanced heat transfer performance

To explore the applicability of NEILs as a potential HTF in CSP system, heat transfer performance was investigated for $[C_4mim][NTf_2]$+1%Al_2O_3 based NEILs. In the present study, heat transfer performances were carried out under forced convection in a circular tube with an inner diameter of 3.86 mm in the laminar flow region. The flow loop (Fig. 2) consisted of a pump, test section, heat exchanger, collection tank, and pressure transducer. The pump was connected to a frequency inverter which was calibrated for the pump using a stopwatch and bucket method. Uniform heat flux was applied to the test section using a flexible heating tape (OMEGA Engg. FGS101-040). Power was supplied to the heater using a DC power (Agilent Technologies: 6655A) supply. To reduce the heat loss to the ambient and to ensure constant heat flux condition, the entire test section was insulated with fiber glass insulation. Five thermocouples were mounted on the tube surface to measure surface temperature. Another two thermocouples were inserted into the tube to measure inlet and outlet liquid temperatures. All thermocouples and pressure transducer were connected to a National Instrument (NI) data acquisition system cDAQ-9178 via a temperature card NI 9211 and pressure card NI 9203 which were interfaced with a computer. Labview software was used for recording all data.

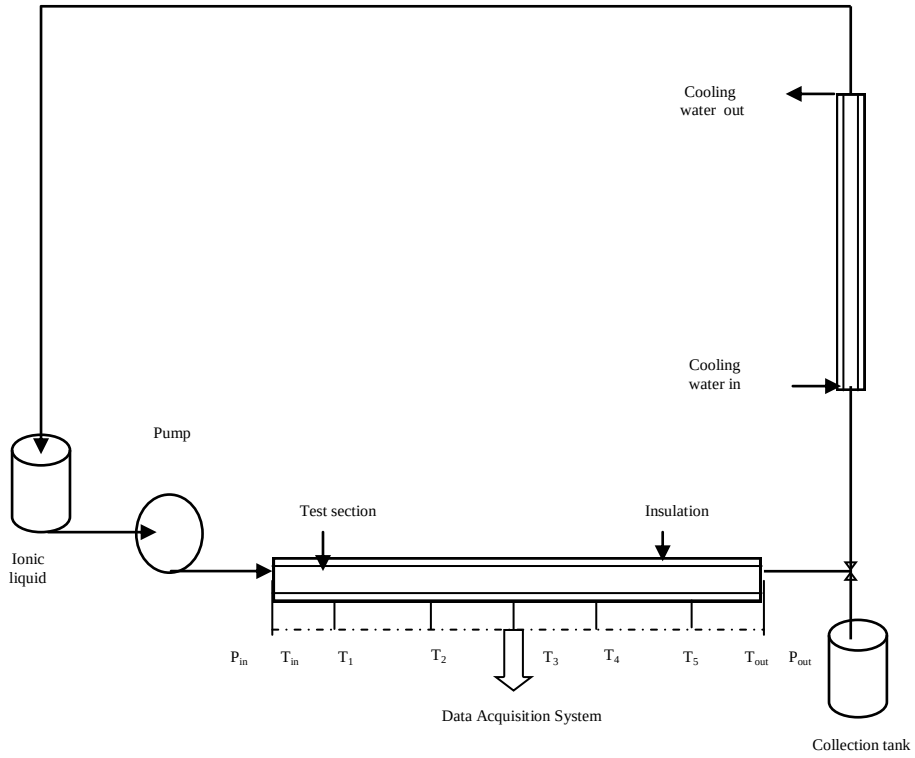

Figure 2: Schematic of the forced convection experimental setup

Fig. 3 shows the local heat transfer coefficient of the 1 % NEIL and base IL as a function of axial distance for $\boldsymbol{Re = 409}$, where $\boldsymbol{Re}$ is the dimensioless Reynolds number. It is clear from Fig. 3 that the NEIL has higher heat transfer coefficient than base IL. Possible reason of this enhancement most probably the mixing effect of particles near the wall, thermal conductivity enhancement, particle migration, and reduction of boundary layer thickness. This enhancement of heat transfer coefficient of NEIL indicates that the NEIL will perform better as HTF compare to base IL.

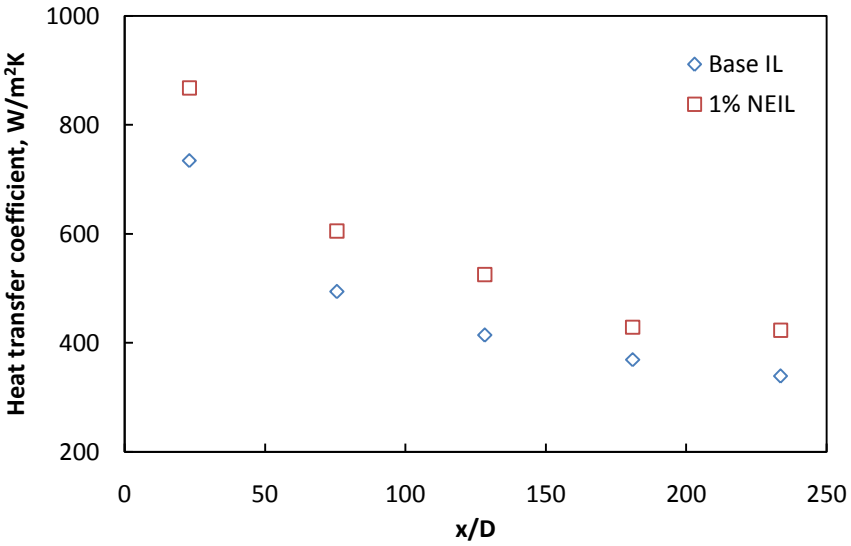

Figure 3: Local heat transfer coefficient along the axial distance, ($Re = 409$)

4. CONCLUSIONS

In this study, the thermal conductivity and heat capacity of base ILs and NEILs made of 1-butyl-3-methylimidazolium bis{(trifluoromethyl)sulfonyl}imide ([C_4mim][NTf_2]) and N-butyl-N-methylpyrrolidinium bis{trifluoromethyl) sulfonyl} imide ([C_4mpyrr][NTf_2]) and 1% Al_2O_3 are measured. The results show that the thermal conductivity is enhanced by ~6% (for [C_4mim][NTf_2]) and ~5% (for [C_4mpyrr][NTf_2]) over the measured temperature range and heat capacity is enhanced by ~23% over the measured temperature range. Moreover, heat transfer coefficient is increased by ~20%. These preliminary findings are favourable to consider NEILs as a potential HTF in solar collector.

.

ACKNOWLEDGEMENTS

The financial support for this research is from Department of Energy (DOE) Solar Energy Technology Program. Savannah River National Laboratory is operated by Savannah River Nuclear Solutions. This document was prepared in conjunction with work accomplished under Contract No. DEAC09-08SR22470 with the U.S. Department of Energy.

REFERENCES:

[1] Bosatra, M., Fazi, F., Lionetto, P. F., Travagnin, L., 2010. Utility Scale PV and CSP Solar Power Plants Performance, Impact on the Territory and Interaction with the Grid, Foster Wheeler Italiana – Corsico (Milan- ITALY).
[2] Bridges, N. J., Visser, A. E. and Fox, E. B., 2011. Potential of Nanoparticle-Enhanced Ionic Liquids (NEILs) as Advanced Heat-Transfer Fluids, Energy Fuels, 25 (10), pp 4862–4864.
[3] Paul, T. C., Morshed, AKM M., Fox, E. B., Visser, A. E., Bridges, N. J., Khan, J. A., 2012. Heat Transfer and Flow Behavior of Nanoparticle Enhanced Ionic Liquids (NEILs), Proceedings of the ASME Summer Heat Transfer Conference, HT2012, Puerto Rico, USA.

[4] Paul, T. C., Morshed, AKM M., Fox, E. B., Visser, A. E., Bridges, N. J., Khan, J. A., 2012. Natural Convection in Rectangular Cavity with Nanoparticle Enhanced Ionic Liquids (NEILs), Proceedings of the International Mechanical Engineering Congress and Exposition IMECE2012, Houston, Texas, USA.
[5] Rogers R. D. and Seddon, K. R., 2003. Ionic liquids–solvents of the future? Science 302, 792–793.
[6] Rooney, D., Jacquemin, J. and Gardas, R., 2009. Thermophysical Properties of Ionic Liquids, Topics in Current Chemistry 290, 185–212.
[7] Kosmulski, M., Gustafsson, J., Rosenholm, J. B., 2004. Thermal stability of low temperature ionic liquids revisited Thermochimica Acta 412, 47–53.
[8] Paul, T. C., Morshed, AKM M., Fox, E. B., Visser, A. E., Bridges, N. J., Khan, J. A., 2011. Experimental Investigation of Natural Convection Heat Transfer of an Ionic Liquid in a Rectangular Enclosure Heated from Below Proceedings of the International Mechanical Engineering Congress and Exposition IMECE2011, Colorado, USA
[9] Wu, B., Reddy, R. G., Rogers, R. D., 2001. Novel Ionic Liquid Thermal Storage for Solar Thermal Electric Power System, Proceedings of Solar Forum-2001, Solar Energy: The Power to Choose, Washington, DC.
[10] Moens, L., Blake, D. M., Rudnicki, D. L., Hale M. J., 2003. Advanced Thermal Storage Fluids for Solar Parabolic Trough Systems, ASME Journal of Solar Energy Engineering, Vol. 125.
[11] Van Valkenburg, M. E. Vaughn, R. L., Williams, M., Wilkes, J. S., 2005. Thermochemistry of ionic liquid heat-transfer fluids, Thermochimica Acta 425, 181–188.
[12] Nieto de Castro, C. A., Lourenco, M. J. V., Ribeiro, A. P. C., Langa, E. and Vieira, S. I. C., 2010. Thermal Properties of Ionic Liquids and IoNanofluids of Imidazolium and Pyrrolidinium Liquids, Journal of Chemical Engineering Data 55, 653–661.
[13] Nieto de Castro, C.A., Murshed, S.M.S., Lourenço, M.J.V., Santos, F.J.V., Lopes, M.L.M., França, J.M.P., 2012. Enhanced thermal conductivity and specific heat capacity of carbon nanotubes ionanofluids, International Journal of Thermal Sciences, Article in press.
[14] Wittmar, A., Ruiz-Abad, D., Ulbricht, M. 2012. Dispersions of silica nanoparticles in ionic liquids investigated with advanced rheology, Journal of Nanoparticle Research, Vol. 14, No. 2. pp. 1-10.
[15] Wang, B., Wang, X., Lou, W., Hao, J., 2011. Ionic liquid-based stable nanofluids containing gold nanoparticles, Journal of Colloid and Interface Science 362, 5–14.
[16] Wang, B., Wang, X., Lou, W., Hao, J., 2011. Gold-ionic liquid nanofluids with preferably tribological properties and thermal conductivity, Nanoscale Research Letters, 6:259.
[17] Wang, B., Wang, X., Lou, W., Hao, J., 2010. Rheological and Tribological Properties of Ionic Liquid-Based Nanofluids Containing Functionalized Multi-Walled Carbon Nanotubes, Journal of Physical Chemistry C 114, 8749–8754.
[18] Shin, D., Banerjee, D., 2011. Enhanced Specific Heat of Silica Nanofluid, Journal of Heat Transfer, Vol. 133 / 024501.
[19] Shin, D., Banerjee, D., 2011. Enhancement of specific heat capacity of high-temperature silica-nanofluids synthesized in alkali chloride salt eutectics for solar thermal-energy storage applications" International Journal of Heat and Mass Transfer 54, 1064–1070.
[20] Maxwell, J. C., 1981. A Treatise on Electricity and Magnetism, 3rd ed.; Clarendon Press: Oxford, UK.
[21] Zhoua S.-Q., Ni, R., 2008. Measurement of the specific heat capacity of water-based Al_2O_3 nanofluid, Applied Physics Letters 92, 093123.

Available online at www.sciencedirect.com

SciVerse ScienceDirect

Procedia Engineering 00 (2012) 000–000

Procedia Engineering

www.elsevier.com/locate/procedia

5th BSME International Conference on Thermal Engineering

Energy efficient wind turbine system based on fuzzy control approach

Altab Hossain[a,*], Ramesh Singh[a], Imtiaz A. Choudhury [a], Abu Bakar [a]

[a]*Department of Enginering Design and Manufacture, Faculty of Engineering, University of Malaya, Kuala Lumpur 50603, Malaysia*

Abstract

Both air flow mechanics and control system of a wind turbine play an important role in its energy management system. Energy is considered as the essential part for the national development in the form of mechanical power or any other which has major contribution for improving the quality of life and enhancing the economic growth. Subsequently, power generation by wind velocity is a complex process with many interacting factors such as wind velocity, climate condition, natural disaster, control system, design structure, vane tip speed ratio, centrifugal force, rotor drag, turbulence flow, roughness and wind shear, etc. Various procedures have been reported in literature to achieve an optimal performance and system effectiveness. However, these control methods had depended only on exact mathematical modelling or on expert's knowledge that can't be relied on solely in modelling such a complex management of air flow mechanics due to its unstable climate condition and so on. In the proposed study, an integrated control model using an adaptive neuro-fuzzy inference system for wind turbine power management strategy has been introduced. In this model, an artificial neural network is employed to develop the fuzzy expert system in order to achieve a more realistic evaluation of wind power extraction. Simulations and experiments have been carried out to investigate the effect of control strategy parameters of the wind turbine and its power extraction.

Keywords: *Renewable energy; Wind velocity ; Fuzzy logic; Power extraction*.

1. Introduction

Energy is considered as the essential part for the national development in the form of mechanical power or any other which has major contribution for improving the quality of life and enhancing the economic growth. Thus, the use of wind turbine in the form of a renewable energy has become as one of the most viable alternative resource of power generation due to some compensations of it such as cost-effective and eco-friendly [1-2]. Various institutions, companies, researchers and organizations have reported that wind turbines with higher efficiency are important to fulfill the energy demand at present [3-4]. The study shows that the efficiency of the wind turbine can be achieved by using optimum turbine parameters in which energy is produced, used and saved. Therefore, a considerable amount of research studies has been devoted to using wind turbines in electricity generation [5-6]. Although, the investigations have shown a reasonably good management of air flow or distribution of wind power generation, the most common controls to improve overall system efficiency of wind turbine are power absorption by reducing the number of losses and hence, more power extraction. Moreover, power absorption is limited by passive stall regulation, which could be controlled by the high load capacity generator. There are several techniques reported in literature to reach an optimum performance and system efficiency by using a conventional control system such as proportional-integral-derivative (PID). However, during the application, correct selection of turbine parameters is critical for estimating the wind power generation by using PID since it depends only on exact mathematical

* Corresponding author. Tel.: +6-03-7967 4448; fax: +6-03-7967 5330.
E-mail address: altab75@um.edu.my; altab76@gmail.com

modeling. Subsequently, power generation in wind turbine device is a complex phenomenon with many other interacting factors such as wind velocity, climate condition, natural disaster, rotor drag, turbulence flow, roughness and wind shear, etc. Hence, there is a need for a more efficient and easier to use a system that could be employed in modeling such a complex management of air flow mechanics. Various techniques have been proposed in the literature [7-9] to predict the wind power by performing field testing, which could be expensive and time consuming as well as using theoretical data based on assumptions. This in turn would affect the accuracy of the developed models in the prediction of wind power. To confront this issue, researchers explored the use of neural network, genetic algorithms and so on, which have been used successfully in numerous engineering fields [10-11]. In this regard, a fuzzy expert system (FES) has become a popular model that offers nonlinear system, and it has the advantage of fuzzy experts not requiring a precise mathematical model. Therefore, the inappropriate and inexact nature of the wind velocity-nonlinear system for a wind turbine could be effectively captured using fuzzy logic, which is considered as a logical system closer to human knowledge and machine language [12]. Therefore, an integrated intelligent model for wind turbine power management scheme is proposed in this study by using an adaptive neuro-fuzzy inference system (ANFIS). In this model, an artificial neural network is employed to develop the fuzzy expert system in order to achieve a more realistic evaluation of wind power extraction. In addition, demonstration is performed to investigate the effect of control strategy parameters on the system performance of the wind turbine and its power extraction.

2. Methodology

2.1. Theoretical analysis

The research has been carried out based on a theoretical analysis for a small-scale vertical axis wind turbine along with the formulation of the mathematical model, optimization of the design parameters of the wind turbine structure and air-flow system. The mathematical model has been formulated by understanding the wind nature, analysing the mechanics of turbine blade-wind interaction and the interaction of air-flow-aerodynamics. The mathematical model is then used for simulating the system performance, optimizing the design parameters and wind power generation. Two kinds of air-flow model have been employed in simulating the aerodynamics of the wind turbine. One is the overall flow model, and the other is a local flow model. The overall flow model is based on a double multiple-streamtube model, including flow expansion in the lateral direction. Moreover, the blade tip effects are significantly important in this model in order to use Prandtl lifting theory. This model is well suited for design investigation due to its reliable output results. On the other hand, the local flow model is based on one blade section conformal recording placed into a circle. Moreover, this analytical model is employed with input data in terms of lift force and pitching moment. The present analytical model is well suited for a design investigation due to the distribution of local pressure without any extra computation time.

Development of an integrated mechanics of turbine-blade-air flow interaction is relatively straightforward conceptually, but somewhat complex to implement and remains a technical challenge since they require many iterative calculations. Especially, theoretical analyses of the turbine blade element and actuator cylinder could be complicated due to the fact that the blades rotate relative to the rotor radius and air flow. To get stable rotational movement of the blade, multiple-streamtube analysis has been conducted such as the determination of lift and drag forces, respectively and hence, shaft torque, output power and power efficiency of the rotor are to be determined [13]. Furthermore, the belt drive system is to be employed, which consists of several parts of the belt drive calculation. Thus, the main calculation that has been done at this system based on angle of wrap for small and large pulley, belt length, pulley speed, the tension ratio and the power transmitted by the belt. In addition, Reynolds number and angle of attack have also been incorporated in order to obtain reasonably good air flow characteristics. Finally, the available wind energy and wind power of the turbine are calculated by making use of the force it exerts on solid objects, pushing them along. Subsequently, windmill blades are designed to move in response to this force and hence, wind machines can extract a substantial portion of the energy and power available. The details have been explained elsewhere published by the authors [13]. The available wind power of the turbine is calculated as the rate of change of kinetic energy of the wind according to the following relationship [9]:

$$P_{wind} = \frac{d\left(\frac{1}{2}mv_{\infty}^{2}\right)}{dt} = \frac{1}{2}v_{\infty}{}^{2}\dot{m} = \frac{1}{2}v_{\infty}{}^{2}\,\rho_{\infty}v_{\infty}S_{T} = \frac{1}{2}\rho_{\infty}S_{T}v_{\infty}{}^{3} \tag{1}$$

where ρ_{∞} is the density of air in kg/m^3, m is the mass of air in kg, $\dot{m}$ is the mass flow rate of air in kg/s, S_T is the total frontal area in m^2, and v_{∞} is the free stream wind velocity in m/s.

The power coefficient (rated power), C_P is calculated as the ratio of power delivered (P) by the system to the total power available on the cross sectional area of the wind stream (P_{wind}) subtended by the wind turbine according to the following relationship.

$$C_P = \frac{P}{P_{wind}} \tag{2}$$

It is noted that for turbines with large total blade area, the change in pressure and the reduction in wind stream velocity will be large but the volumetric flow rate of the wind stream will be low which results in a lower power output and hence a low power coefficient.

Using equations of state for perfect gas the air density, ρ_∞ is defined as [14]:

$$\rho_\infty = \frac{p}{RT} \tag{3}$$

where p is the absolute pressure in N/m^2, T is the temperature in K, and R is the gas constant of air in Nm/(kgK).

Reynolds number (Re) based on the chord length is defined as [14]:

$$\mathrm{Re} = \frac{\rho_\infty v_\infty c}{\mu_\infty} \tag{4}$$

where v_∞ is the free stream wind velocity in m/s; μ_∞ is the dynamic viscosity in kg/ms, and c is the chord length in m. The chord length of the blade is considered as 139.7 mm.

The air viscosity μ_∞ is determined using the Sutherland's equation described below [15]:

$$\mu_\infty = 1.458\times10^{-6}\frac{T^{1.5}}{T+110.4} \tag{5}$$

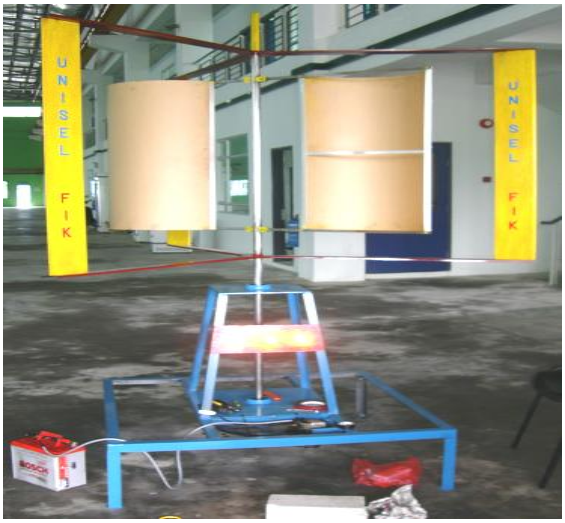

Fig. 1. Illustration of the vertical axis wind turbine used to measure the power generation.

2.2. Wind turbine model development and testing

A small scale energy efficient vertical axis wind turbine (VAWT) (Fig. 1) was developed and tested. Details of the wind turbine development were presented elsewhere [13]. The top and bottom of each blade was a 1066.8 mm x 139.7 mm x 50.8 mm deep rectangular section to allow for easier connections to the radial arms and passive pitching system. The shaft was

connected to the main parts and to the alternator during the full assembly of this vertical axis wind turbine. The belt drive system was consisted of several parts of the belt drive calculation and the V–Type belt was considered. The corner sharp had been used as aerofoil for the wind turbine blade by producing a controllable aerodynamic force with its motion through the wind flow. The components of the small scaled vertical axis wind turbine are designed by using the CATIA software installed in the Structural Laboratory. VAWT generated the power via a combination of turbine blade-air flow interaction and electric generators. In general, as the rotor rotates it converts the wind energy into mechanical energy. Several experiments were carried out in an open area of the laboratory. Before starting the operation, the battery terminal and alternator terminal were checked and connected to the light bulbs via connecting switch. Due to the rotation of the wind turbine blade, current was produced and the bulbs were turned on. The ambient pressure and temperature were recorded using the manometer and thermometer, respectively for the evaluation of air density in the laboratory environment. The power produced by the wind speed was also calculated by using equations (1-6). The wind speeds at the time of testing was measured between 5.89 and 7.02 m/s by using a digital manometer. For the different measured velocities, corresponding Reynolds numbers and wind power were calculated. The simulations had been carried out by using MATLAB for wind power measurement.

2.3. Adaptive Neuro-Fuzzy Inference System (ANFIS)

ANFIS is a fuzzy inference system implemented in the framework of adaptive networks by Jang [10]. ANFIS is an integrated intelligent model, where an artificial neural network is employed to develop the fuzzy expert system in order to achieve a more realistic evaluation of wind power extraction as shown in Fig. 2. The ANFIS model proposed in this paper has a total of five layers and two inputs, Reynolds number (RE) and wind velocity (WV), and one output wind power generation (WP) have been considered for the convenience of modelling. In general, a neuro-fuzzy system is a neural network which is functionally equivalent to a fuzzy-inference system (FIS). For fuzzification, the linguistic variables very low (VL), low (L), medium (M), high (H), and very high (VH) are used for the inputs and output. The units of the used factors are: RE (-), WV (m/s) and WP (W). For the two inputs and one output, a fuzzy associated rule is developed as shown in Table 1. Total of 25 rules were formed by the ANFIS.

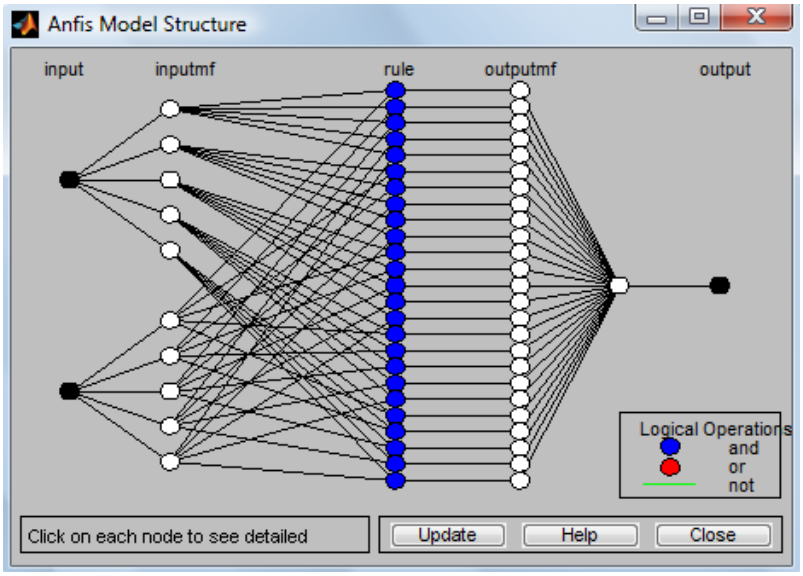

Fig. 2. The structure model found from the ANFIS.

Table 1. Rules found from ANFIS

RE \ WV	VL	L	M	H	VH
VL	VL	VL	VL	VL	L
L	VL	L	M	M	H
M	M	M	M	M	H
H	M	M	H	H	H
VH	M	H	H	VH	VH

3. Results and Discussions

The fuzzy logic toolbox in MATLAB was used to develop FIS and to train the ANFIS model in order to achieve the maximum prediction accuracy. Finally, control surface had been developed based on ANFIS model (Fig. 3). The fuzzy control surface for the set associations described in the preceding sections have been incorporated in this figure where the output variable "WP". It depicts the non-linear surface of the Sugeno Fuzzy model for the wind power generation prediction problem. It may serve as visual depiction of how the intelligent system operates dynamically over time. This is the mesh plot of the example relationship between WV and RE on the input side and model output WP on the output side and displays the range of possible defuzzified values for all possible inputs. The plot is used to check the rules and the membership functions and to see if they are appropriate and whether modifications are necessary to improve the output until the output curves are desired. The result in Fig. 3 shows that the surface represents in a compact way all the information in the fuzzy logic expert system. Hence, it can be noted that this representation is limited in that if there are more than two inputs it becomes difficult to visualize the surface. Furthermore, this figure simply represents the range of possible defuzzified values for all possible inputs WV and RE. It also shows that as the wind velocity (WV) and Reynolds number (RE) increased, there is concomitant increased in wind power generation (WP) and vice versa [8-9]. It shows that wind power generation reached a peak when the wind velocity and Reynolds number both reached their respective maximum level, although the effect is less prominent at the lower level of air density used in Reynolds number calculation since air density is very low and wing cord length have been considered as constant in the device. Consequently, wind power generation decreased to its lowest value when wind velocity and Reynolds number both reached their respective minimum level. It should be noted that the model's core objective is to predict the wind power generation within considerable limits of ambiguity. The prediction of wind power generation is dependent on the system variables that may vary time to time and place to place. Increasing the number of input variables would certainly improve the precision of wind power prediction. However, in this case the base of the fuzzy rules can be extensively complex, and the improvement of the output variable will still be small. Furthermore, it would increase the computational time.

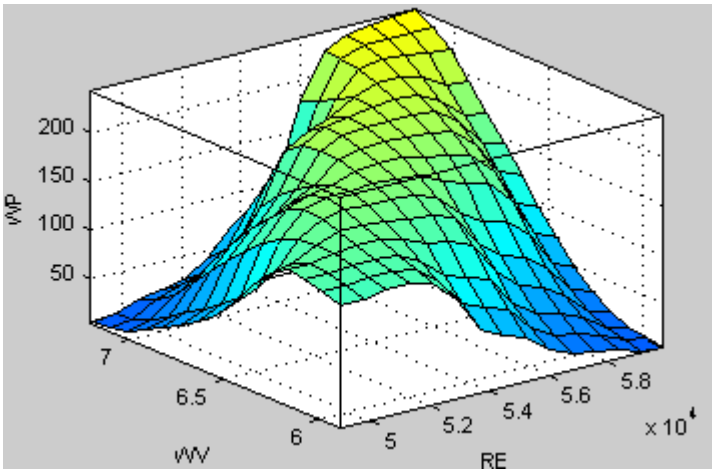

Fig. 3. Control surface of the fuzzy inferring system: WP (W), WV (m/s), RE (-).

4. Conclusions

In this research, an adaptive neuro-fuzzy inference system (ANFIS) is proposed to predict wind power generation. A small scale vertical axis wind turbine is used to simulate the performance of the developed model. Furthermore, demonstration has been performed to investigate the effect of ANFIS model on the system performance of the wind turbine and its power extraction. This work has demonstrated the viability of the developed ANFIS model to evaluate power genertaion in wind turbine within high accuracy without needing to undergoing laborious experimental work for a variety of environmental conditions with many uncertanties which can be noneconomical and time consuming. Future work is ongoing with the development of full scale wind turbine along with other novel control techniques.

Acknowledgements

The authors are grateful for the support provided by University Selangor (UNISEL) for this project.

References

[1] Hansen, A. D., Iov, F., Blaabjerg, F. & Hansen, L. H., 2004. Review of Contemporary Wind Turbine Concepts and their Market Penetration. *Journal of Wind Engineering*, *28*(3) 247-263.
[2] Keith, D.W., 2005. The Influence of Large-Scale Wind Power on Global Climate. *Proc. of the National Academy of Sciences*, Washington D.C, 101, 12−56.
[3] Musgrove, P.J., 1987. Wind Energy Conversion: Recent Progress and Future Prospects. *Solar and Wind Technology*, *4*(1) 37−49.
[4] Hansen, A. D., Sorensen, P., Iov, F. & Blaabjerg, F., 2006. Centralised power control of wind farm with doubly fed induction generators, *Journal of Renewable Energy*, *31*, 935-951.
[5] Robinson, M. L., 1981. The Darrieus Wind Turbine for Electrical Power Generation. *J. Royal Aeronautical Society*, *85*, 244-255.
[6] Eriksson, S. & Bernhoff, H., 2005. Generator-damped Torsional Vibrations of a Vertical Axis Wind Turbine. *Wind Engineering*, *29*(5) 449–462.
[7] Sun, T., Chen, Z. & Blaabjerg, F., 2005. Transient Stability of DFIG Wind Turbines at an External Short-circuit-Fault. *Wind Energy*, *8*, 345-360.
[8] Kusiak, A., Zheng, H. & Song, Z., 2009. Wind Farm Power Prediction: A Data-Mining Approach. *Wind Energ.*, *12*, 275–293.
[9] Barbounis, T. G., Theocharis, J. B. & Alexiadis, M. C., 2006. Dokopoulos PS. Long-term wind speed and power forecasting using local recurrent neural network models. *IEEE Transactions on Energy Conversion*, *21*, 273–284.
[10] Jang, J. S. R., 1993. ANFIS: adaptive-network-based fuzzy inference system. *IEEE Transactions on Systems, Man and Cybernetics*, *23*(3), 665-684.
[11] Hossain, A., Rahman A. & Mohiuddin. A. K. M., 2011. Fuzzy Expert System for Controlling Swamp Terrain Intelligent Air-Cushion Tracked Vehicle. *International Journal of Automotive Technology*, *12*(5) 745-753.
[12] Hossain, A., Rahman, A., Rahman, M., Hassan, Sk. & Hossen, J., 2009. Prediction of Power Generation of Small Scale Vertical Axis Wind Turbine Using Fuzzy Logic. *J. Urban and Environmental Engineering*, *3*(2),43−51.
[13] Hossain, A., Iqbal, A.K.M.P., Rahman, A., Arifin, M. & Mazian, M., 2007. Design and Development of A 1/3 Scale Vertical Axis Wind Turbine for Electrical Power Generation. *J. Urban and Environmental Engineering, 1*(2), 53−60.
[14] Bertin J. J. (2002) *Aerodynamics for the Engineer*, New Jersey, Prentice Hall, Inc., U.S.A
[15] Anderson .J..D.Jr. (1999) *Aircraft Performance and Design*, McGraw Hill Companies Inc., U.S.A.

Appendix A. An example of fuzzification

The first block inside the fuzzy expert system (FES) is fuzzification, which converts each piece of input data to degrees of membership by a lookup in one or several membership functions. The fuzzification block thus matches the input data with the conditions of the rules to determine how well the condition of each rule matches that particular input instance. There is a degree of membership for each linguistic term that applies to that input variable.

Fuzzifications of the used factors were made by aid follows functions. These formulas were determined by using measurement values.

$$RE(i_2) = \begin{Bmatrix} i_2; 4.88 \le i_2 \le 6.0 \\ 0; otherwise \end{Bmatrix}$$

$$WV(i_1) = \begin{Bmatrix} i_1; 5.9 \le i_1 \le 7.24 \\ 0; otherwise \end{Bmatrix}$$

Rule 1 and 15 can be interpreted as follows.

Rule 1: If Reynolds number (RE) is VL and wind velocity (WV) is VL, then wind power (WP) is VL.
Rule 15: If Reynolds number (RE) is M and wind velocity (WV) is VH, then wind power (WP) is H.

Available online at www.sciencedirect.com

SciVerse ScienceDirect

Procedia Engineering 00 (2012) 000–000

Procedia Engineering

www.elsevier.com/locate/procedia

5th BSME International Conference on Thermal Engineering

A comparative study on pyrolysis for liquid oil from different biomass solid wastes

Mohammad Nurul Islam [a,*], Uzzal Hossain Joardder[b], SM Nazmul Hoque[b] and Md. Shazib Uddin[b]

[a,*]*Department of Mechanical Engineering, Institute Technology Brunei, Jalan Tungku Link, Gadong, BE 1410, Brunei Darussalam*
[b]*Department of Mechanical Engineering, Rajshahi University of Engineering and Technology, Rajshahi 6204, Bangladesh*

Abstract

Locally available different biomass solid wastes, pine seed, date seed, plum seed, nutshell, hay of catkin, rice husk, jute stick, saw-dust, wheat straw and linseed residue in the particle form have been pyrolyzed in laboratory scale fixed bed reactor. The products obtained are pyrolysis oil, solid char and gas. The oil and char are collected while the gas is flared into atmosphere. The variation of oil yield for different biomass feedstock with reaction parameters like, reactor bed temperature, feed size and running time is presented in a comparative way in the paper. A maximum liquid yield of 55 wt% of dry feedstock is obtained at an optimum temperature of 500 ^{o}C for a feed size of 300-600µm with a running time of 55 min with nutshell as the feedstock while the minimum liquid yield is found to be 30 wt% of feedstock at an optimum temperature of 400 ^{o}C for a feed size of 2.36 mm with a running time of 65 min for linseed residue. A detailed study on the variation of product yields with reaction parameters is presented for the latest investigation with pine seed as the feedstock where a maximum liquid yield of 40 wt% of dry feedstock is obtained at an optimum temperature of 500 ^{o}C for a feed size of 2.36-2.76 mm with a running time of 120 min. The characterization of the pyrolysis oil is carried out and a comparison of some selected properties of the oil is presented. From the study it is exhibited that the biomass solid wastes have the potential to be converted into liquid oil as a source of renewable energy with some further upgrading of the products.

Keywords: Pyrolysis; biomass; renewable energy; pyrolysis oil; characterization.

1. Introduction

Energy propels the society. It is the major requirement of present society for its sustainable development. The energy consumption in the world has been growing at an alarming rate. By the year 2100, the world population is expected to be more than 12 billion and it is estimated that the demand for energy would increase by five times the present demand [1]. Thus, significant consumption and depletion of fossil fuel and the evident global warming are pressing continuously to think for alternative energy sources. Under such circumstances, it has become imperative to find out some potential sources of energy that may be able to meet considerable part of the energy demand in future. Biomass has been recognized as a major renewable energy source to supplement this declining fossil fuel source of energy [2]. It is considered to be the most popular form of renewable energy. Biomass and its solid waste is attractive from the points of view of ease of availability, high carbon content, low moisture and ash content, low or even no cost, no conflict arising from alternative usage, solving solid waste disposal problems and keeping the environment clean. In some cases, it may have some existing usage; however, the better utilization and application from the point of view of energy recovery and environment need to be emphasized. Currently bio-oil production is becoming very much promising [3]. There are various biomass solid wastes available in

* Mohammad Nurul Islam. Tel.: +673-246-1020 ext.1221; fax: +673-246-1035.
E-mail address: mohammad.islam@itb.edu.bn; mnislam60@yahoo.com

different corners of the world including Bangladesh and Brunei Darussalam. A few examples are: date seed, pine seed, nutshell, wheat straw, linseed residue, hay of catkin, rice straw, bagasse, jute stick, sawdust, rice husk, empty fruit bunches, livestock, scrap tire, refused plastic, wastepaper etc. These carbonaceous solid wastes are renewable energy sources and therefore, the potential of converting them into useful energy such as liquid oil should be seriously considered. In this way, the wastes would be more readily useable and environmentally more acceptable. It is found from the characterization of most of these biomass solid wastes that these wastes contain higher percentage of volatile matter. This high volatile content biomass has high potential for pyrolysis liquid production [4]. Transformation of energy into useful and sustainable forms that can fulfill and suit the requirements of mankind in the best possible way is the common concern of the scientists, engineers and technologists. From the point of view of energy transformation, pyrolysis is more attractive among various thermochemical conversion processes because of its simplicity and higher conversion capability into liquid product. Pyrolysis is generally described as the incomplete thermal degradation of the carbonaceous solid materials in the complete absence of oxygen or oxidizing agent at relatively moderate temperature of 500 to 800°C to yield condensable liquid, known as bio-oil, bio-fuel, bio-crude, char (charcoal) and gaseous products (fuel gases). Pyrolysis system may be either fixed bed or fluidized bed. In fixed bed system, a fixed bed pyrolysis reactor is used. As the feedstock is kept fixed in the reaction bed (reactor), it is called fixed bed pyrolysis. In this process, the feed material is fed into the reactor and heat is applied externally at a faster rate. In this work an external biomass source heater is used. Nitrogen is used as inert gas for making inert atmosphere in the system and for helping the gaseous mixture to dispose of the reactor. From the reactor, the vaporized mixture passes through water-cooled condenser. Extracting heat from the vapor, condenser converts it into liquid product and a part of the vapor is escaped as non-condensable gas. The process of biomass pyrolysis is considered to be very complex consisting of both concurrent and consecutive reactions. A possible reaction pathway of pyrolysis of biomass solid waste is presented in Fig. 1.

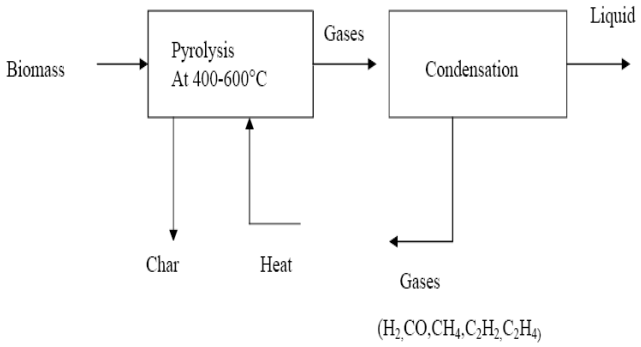

Fig. 1. A possible reaction pathway of pyrolysis of biomass solid waste.

This technology is spreading with research and experimental work in many countries of the present world [5-6]. The pyrolysis oil has moderate heating value, can be easily transported, can be burnt directly in thermal power plant and in gas turbine or can be upgraded to obtain light hydrocarbons for transport fuel and for the production and recovery of chemicals [7]. In this study fixed bed pyrolysis of a number of biomass solid wastes, widely available in Bangladesh is considered to obtain bio-oil, solid char and gases. Thus, the wastes may be used for energy recovery as fuel. It is to mention that there are scopes to upgrade the oil to obtain high grade fuels and valuable chemicals. The solid char can be used for making activated carbon (AC). The char has its potential as a solid fuel as well [7]. AC production costs can be reduced by either choosing a cheap raw material or by applying a proper production method like pyrolysis system [8]. Thus, the pyrolysis conversion appears to be a new development in the alternative renewable sources of energy. Recently UK, Malaysia and India have given much attention towards the pyrolysis technology. A number of pyrolytic conversion studies using different biomass solid wastes has been carried out in the Department of Mechanical Engineering of Rajshahi University of Engineering & Technology. A comparative study on the liquid product yields and their characterization analysis has been taken into consideration in this paper.

2. Materials and methods

2.1. Materials

The feedstock raw-materials collected are pine seed, date seed, plum seed, nutshell, hay of catkin, rice husk, jute stick, saw dust, wheat straw and linseed residue. These are collected locally in Rajshahi and then milled into particles and air-dried. Finally the feedstock is oven-dried at 105-110^{o}C for 24 hours prior to pyrolysis. The proximate analysis of the feedstock is presented in Table 1.

Table 1. Proximate analysis of different feedstock.

Feedstock (%)	Moisture (%)	Volatile (%)	Fixed carbon (%)	Ash (%)
Pine seed	5	-	-	4.5
Date seed	5-10	-	-	1-2
Nut shell	4.6	72.22	21.16	0.56
Plum seed	-	-	-	-
Rice husk	12	52.4	17.1	18.5
Saw-dust	7.5	91	-	1.5
Jute stick	9.02	78.40	11.80	0.78
Wheat straw	5.17	71.32	16.69	6.82
Linseed residue	6.7	77.7	10.7	5.6
Hay of catkin	-	-	-	-

2.2. Experimental

Each of the feedstock is pyrolyzed individually in externally heated stainless steel fixed bed pyrolysis reactor system. The main components of the system are fixed bed reactor, liquid condenser and ice-cooled liquid collectors. The schematic diagram of the fixed bed pyrolysis system is shown in Fig. 2.

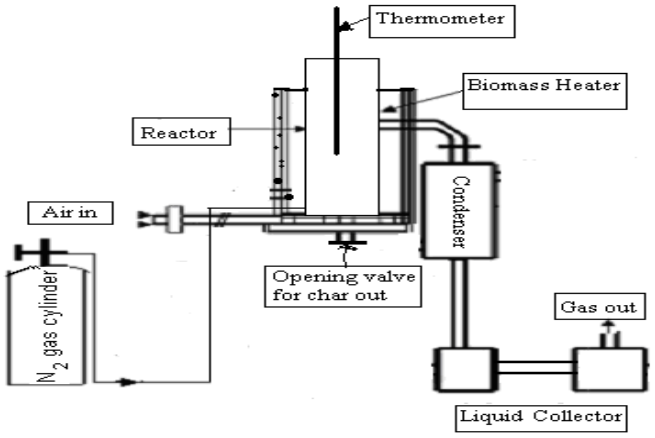

Fig. 2. Schematic diagram of fixed bed pyrolysis system.

The effective dimensions of the reactors are presented in Table 2. The reactor is heated externally by a biomass source heater at different temperatures from 400 to 600^{o}C. The temperature is measured by means of pyrometer and mercury thermometer. Nitrogen gas is supplied in order to maintain the inert atmosphere in the reactor, and to dispose of the pyrolyzed vapor products to the condenser. Pyrolysis vapor is condensed into liquid in the condenser and collected in the ice-cooled liquid collectors. The char is collected from the reactor bed after each experimental run through the opening at the bottom of the reactor. The non-condensable gas is flared into the atmosphere.

3. Results and discussion

3.1. Product yield

The products obtained from the pyrolysis experimental studies are liquid oil, solid char and gas. The products obtained from the latest experimental study using pine seed as the feedstock are shown in Fig. 3.

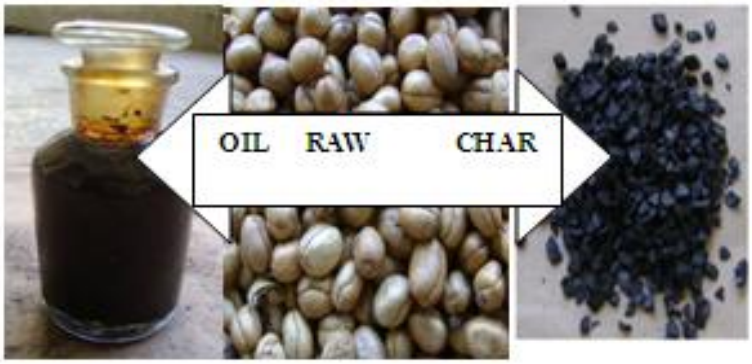

Fig. 3. Products obtained from the pyrolysis of pine seed.

The maximum liquid product yields of different biomass solid wastes for different reactor dimensions and their associated reaction conditions are presented in Table 2.

Table 2. The maximum product yields of different solid waste pyrolysis oils and the corresponding reaction conditions

Biomass	Pine seed	Date seed	Plum seed	Nut shell	Hay of catkin	Rice husk	Jute stick	Saw-dust	Wheat straw	Linseed residue
Reactor dimensions (dia, cm x height cm)	7.6 x 46	7.6 x 46	7.6 x 46	6.0 x 29	6.0 x 29	4.0 x 38	7.0 x 37.6	4.0 x 38	6.0 x 29	6.0 x 29
Liquid product yields (%)	40	50	39	55	44	40	50	41	53	30
Optimum operating temperature (^{o}C)	500	500	520	500	450	450	425	440	500	400
Feed size (μm)	2.36-2.76 mm	0.11-0.20 cm^3	2.36-4.75 mm	300-600	300-600	<1000	420	350-450	300-600	2.36 mm
Running time (min)	120	120	120	55	75	75	60	65	65	65

3.1.1. Effect of operating temperature

The effect of reaction conditions on product yields for the biomass feedstock pine seed, which was the latest experimental study is presented here. The similar trend of product yields is observed for other biomass feedstock as well. The relationship between the variation of percentage of weight of liquid, char, and gaseous products at different reactor bed temperature is presented in Fig. 4. The results show that the liquid yield increases with operating temperature and a

maximum yield of 40 wt %. is obtained at 500 ^{o}C for feed particle size of 2.36-2.76 mm with a running time of 120 min. When the temperature exceeds 500 ^{o}C, liquid yield decreases. At a lower temperature of 400 ^{o}C, the liquid product is found to be 30 wt% of the dry feedstock. The higher temperature may cause secondary cracking reaction of the vapors, yielding more gas products at the cost of liquid product. On the other hand, the reason for the lower liquid yield at lower temperature may be due to insufficient temperature to complete decomposition of the feed material.

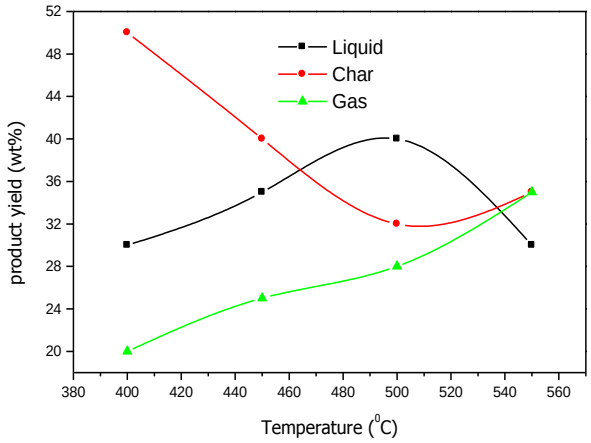

Fig. 4. Effect of operating temperature on product yield.

3.1.2. Effect of feed particle size on product yield

Fig. 5 represents the percentage weight of liquid, solid char and gas products for different feed particle size at a reactor bed temperature of 500 ^{o}C and an operating time of 120 minutes. It is observed that at 500 ^{o}C, the percentage of liquid collection is maximum at 40 wt% of total biomass feed for particle size of 2.36-2.76 mm. Liquid yield is found to be maximum for the smaller particles because the larger size particles might not be adequately heated up so rapidly causing incomplete pyrolysis.

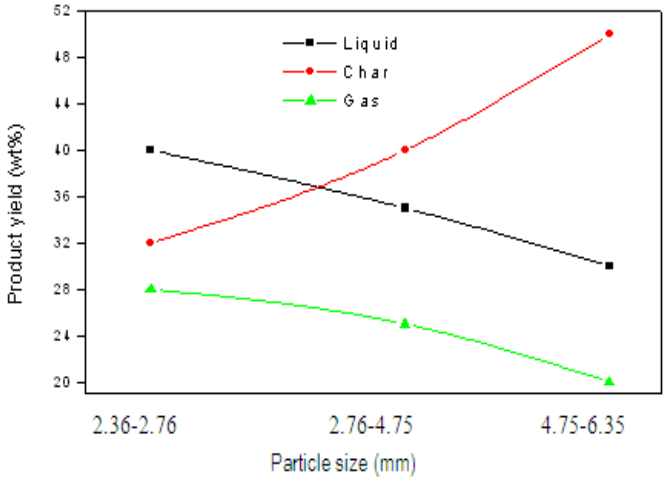

Fig.5. Effect of feed particle size on product yield.

3.1.3. Effect of running time on product yield

Fig. 6 shows the variation of product yield (wt %) of liquid, solid char and gas products with running time at a temperature of 500 ^{o}C for feed particle size of 2.36-2.76 mm. The maximum liquid product is found to be 40 wt% of biomass feed while the solid char product is 32 wt% of dry feed at 120 minutes. It is observed that at lower and higher

running times, the liquid product yields are not optimum that may be due to insufficient pyrolysis reaction and higher rate of gas discharge respectively.

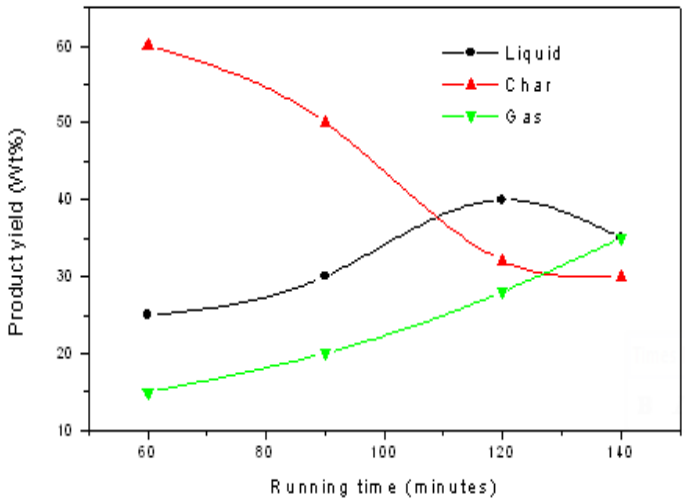

Fig. 6. Effect of running time on product yield.

3.2. Characterization of pyrolysis oil

The characterization of the pyrolysis oil from different biomass solid waste is presented in Table 3. The oil is found to be a dark-color single phase liquid. The energy content of the oil in the form of higher heating value (HHV) is found to vary from 20 to 33 MJ/kg which is certainly higher than the corresponding solid biomass feedstock. Some oils are found to be heavier than water while the others are lighter, the density being in the range of 900 to 1224 kg/m^3. The low viscosity of the pyrolysis oils is a favorable feature for handling and transportation of the liquid oils. The oils are found to be corrosive in nature having pH values in the acidic range. The flash point is found to be reasonable.

Table 3. Comparison of physical properties of pyrolysis oil from different biomass solid waste

Properties	Pine seed	Date seed	Plum seed	Nut shell	Hay of catkin	Rice husk	Jute stick	Saw-dust	Wheat straw	Linseed residue
Kinematic viscosity (cSt)	12.15	6.63	1.14	9.72	10.95	1.20	12.8	0.98	9.85	8.72
Density (kg/m^3)	1166	1042.4	940	900	900	960	1224	910	1098.6	1095
Flash Point (^{0}C)	120	126	112	-	-	-	>70	-	-	-
pH value	-	-	3.19	-	-	2.22	2.92	2.23	-	-
HHV (MJ/kg)	20.00	28.64	22.39	19.34	23.43	20.43	21.09	19.08	17.23	33.35

3.3. Comparison among pyrolysis oil, biomass oil and diesel fuel

Table 4 shows the comparison of some of the fuel properties of pyrolysis oil derived from different biomass solid waste feedstock with diesel and heavy fuel. It is evident that the density and viscosity of pyrolysis oil are favorable and closer to

diesel. The higher heating value of the pyrolysis oil is found to be in the comparable range with other reported pyrolysis oil while still being less than diesel and heavy fuels.

Table 4. Comparison of pyrolysis oil with conventional fuel

Analysis	Pine seed	Date seed	Plum seed	Nut shell	Hay of catkin	Rice husk	Jute stick	Saw-dust	Wheat straw	Linseed residue	Diesel	Heavy fuel oil
Kinematic viscosity at 26^0C (cSt)	12.15	6.63	1.14	9.72	10.95	1.20	12.8	0.98	9.85	8.72	2.61	200
Density (kg/m^3)	1166	1042.4	940	900	900	960	1224	910	1098.6	1095	827.1	980
Flash Point (^{0}C)	120	126	112	-	105	-	>70	-	-	-	53	90-180
HHV (MJ/kg)	20.00	28.64	22.39	19.34	23.43	20.43	21.09	19.08	17.23	33.35	45.18	42-43
pH value	-	-	3.19	-	2.98	2.22	2.92	2.23	-.	-	-	-

4. Conclusions

Biomass solid wastes are successfully converted into liquid oil, solid char and gas by fixed bed pyrolysis system. The maximum liquid yield is found to be the highest of 55 wt% of dry biomass feedstock for nut shell at a temperature of 500 ^{o}C for a feed size of 300-600 µm with a running time of 55 min while the lowest liquid yield is found to be 30 wt% of dry biomass feedstock at a temperature of 400 ^{o}C, for a feed size of 2.36 mm with a running time of 65 min with linseed residue as the feed material. The heating value of the pyrolysis oil is found to be in the range of 20.00 to 33.35 MJ/kg, which is either similar or higher than other biomass derived pyrolysis oils. However, the values are significantly higher than that of the corresponding solid biomass wastes. The density and viscosity of the oil are found to be higher than that of diesel and heavy fuel. Thus, the oil from the biomass solid wastes may be considered to be an important candidate of potential sources of alternative fuel that may further be upgraded.

Acknowledgements

The authors are grateful to Rajshahi University of Engineering Technology and Institute Technology Brunei for providing the facilities to carry out the study and permission to present the paper.

References

[1] Sayigh, A., 1997. "Renewable energy- the way forward," International Symposium on Advances in Alternative Energy 1997. Johor Bahru, Malaysia, keynote paper.

[2] Williams, P.T., Halim, S., Taylor, D.T., 1992. Pyrolysis of Oil Palm Solid Waste, in *"Biomass, Energy, Industry and Environment"* Grassi G, Collina A, Zibetta H., Editors. Elsevier Applied Science, London, p. 757.

[3] Islam, M.N., Ani, F.N.,1998. Characterization of bio-oil from palm shell pyrolysis with catalytic upgrading," World Renewable Energy Congress, Elsevier Science, pp. 1977-1999.

[4] Islam, M.N., 1999. Pyrolysis of Biomass Solid Waste and Its Catalytic Treatment along with Economic Analysis. Ph. D. Thesis, Faculty of Mechanical Engineering, Universiti Teknologi Malaysia, Malaysia.

[5] Bridgewater, A.V., Bridge, S.A., 1991. A Review of Biomass Pyrolysis and Pyrolysis Technologies, in *Biomass Pyrolysis Liquids Upgrading and Utilization*, Bridgwater, A.V., Grassi, G., Editors. Elsevier Applied Science, London, p. 11.

[6] Marshall, A.T., Morris, J.M., 2006. A Watery Solution and Sustainable Energy Parks. CIWM Journal, August, 2006.

[7] Horne, P.A., Williams, P.T., 1994. Petroleum Quality Fuels and Chemical from the Fluidized Bed Pyrolysis of Biomass with Zeolite Catalyst Upgrading. Renewable Energy 5(2), p. 810.

[8] Lafi, W.K., 2001. Production of Activated Carbon from Acorns and Olive Seeds. Biomass and Bioenergy. 20, p. 57.